HAL
open science

Improvement of the Calculation Accuracy of Acid Gas Solubility in Deep Reservoir Brines: Application to the Geological Storage of CO2

C. Kervévan, Mohamed Azaroual, P. Durst

To cite this version:

C. Kervévan, Mohamed Azaroual, P. Durst. Improvement of the Calculation Accuracy of Acid Gas Solubility in Deep Reservoir Brines: Application to the Geological Storage of CO2. Oil & Gas Science and Technology - Revue d'IFP Energies nouvelles, 2005, 60 (2), pp.357-379. 10.2516/ogst:2005022 . hal-02017199

HAL Id: hal-02017199

https://hal.science/hal-02017199v1

Submitted on 13 Feb 2019

HAL is a multi-disciplinary open access archive for the deposit and dissemination of scientific research documents, whether they are published or not. The documents may come from teaching and research institutions in France or abroad, or from public or private research centers.

L'archive ouverte pluridisciplinaire **HAL**, est destinée au dépôt et à la diffusion de documents scientifiques de niveau recherche, publiés ou non, émanant des établissements d'enseignement et de recherche français ou étrangers, des laboratoires publics ou privés.

Oil & Gas Science and Technology – Rev. IFP, Vol. 60 (2005), No. 2, pp. 357-379
Copyright © 2005, Institut français du pétrole

IFP International Workshop
Rencontres scientifiques de l'IFP

Gas-Water-Rock Interactions ... / Interactions gaz-eau-roche ...

Improvement of the Calculation Accuracy of Acid Gas Solubility in Deep Reservoir Brines: Application to the Geological Storage of CO_2

C. Kervévan[1], M. Azaroual[1] and P. Durst[1]

1 BRGM, Hydrological and Hydrochemical Modelling, Water Division, 3, avenue C. Guillemin, BP 6009, 45060 Orléans Cedex 2 - France
e-mail: c.kervevan@brgm.fr - m.azaroual@brgm.fr - p.durst@brgm.fr

Résumé — Amélioration de la précision du calcul de la solubilité des gaz acides dans les saumures des réservoirs profonds : application au stockage géologique du CO_2 — L'évaluation des conséquences à court et long terme de l'injection de CO_2 dans les aquifères nécessite à la fois des expérimentations en laboratoire et l'utilisation de modèles afin de mieux comprendre les différents processus physicochimiques induits. La modélisation de l'injection dans un réservoir où les conditions *in situ* sont souvent relativement élevées en termes de température (au-delà de 50 °C), pression (plusieurs centaines de bars) et salinité (supérieure à celle de l'eau de mer), implique donc d'avoir à notre disposition des outils numériques capables de prendre en compte à la fois les effets spécifiques de chaque électrolyte et la non-idéalité de la phase CO_2 gaz. Cet article propose une évaluation de la cohérence des différentes corrections (activité, fugacité, influence de la pression sur les constantes thermodynamiques) à considérer dans les modèles géochimiques afin de répondre aux besoins en termes de précision de calcul. Ces corrections ont été introduites dans le logiciel de modélisation thermo-cinétique SCALE2000 (Azaroual *et al.*, 2004a), utilisé pour tester leur validité en comparant les résultats de calcul à des données expérimentales ou à des résultats d'autres modèles concernant la solubilité du CO_2. Une estimation du poids relatif de chacune des corrections, dans le cas d'une saumure de salinité égale à 237 $g \cdot l^{-1}$ (60 °C, $pCO_2 = 200$ bar), montre une surestimation systématique de la solubilité du CO_2 (supérieure à 100 %) lorsque la salinité (NaCl équivalente) est négligée ou que le gaz est considéré comme idéal ; en comparaison, l'erreur induite en considérant l'équivalent NaCl au lieu de la salinité réelle de la saumure est faible (moins de 5 %).

La deuxième partie de cette étude présente un exemple d'application à un scénario hypothétique d'injection massive de CO_2 dans un réservoir carbonaté ; les données utilisées pour la composition de la saumure correspondent à des données réelles (Moldovanyi et Walters, 1992) provenant de la formation de Smackover (Arkansas, États-Unis). Les simulations réalisées en considérant un volume élémentaire représentatif de roche saturée (assemblage minéral poreux saturé avec la saumure de Smackover), soumis à une pression de CO_2 constante de 150 bar, montrent deux comportements distincts selon que le système est supposé fermé (réacteur *batch*) ou ouvert et alimenté par un flux constant de saumure. Dans le premier cas, les calculs réalisés avec SCALE2000 aboutissent à une modification négligeable de la composition minéralogique. Dans le second cas, plus représentatif du caractère dynamique d'un système d'injection, les résultats montrent des modifications majeures de la minéralogie aboutissant finalement à une forte augmentation de la porosité (passant de 20 % initialement à 85 % après 50 ans simulés).

Une nouvelle série de calculs a ensuite été réalisée avec SCALE2000, en considérant cette fois un système 1D constitué d'un assemblage en série de quatre réacteurs homogènes identiques (vitesse du

fluide de 1 m·jour^{-1}). Avec des conditions initiales et aux limites similaires à celles utilisées précédemment et en imposant pCO_2 uniquement dans le premier réacteur, les résultats obtenus ont montré que la dolomite précipitait en quantité significative dans le réacteur le plus aval du système, induisant, par voie de conséquence, la précipitation de CO_2. Des premiers calculs de bilan de masse réalisés sur le système des quatre réacteurs ont finalement démontré une perte globale en carbone minéral par rapport aux quantités initialement présentes. Toutefois, les tendances des évolutions observées dans les deux réacteurs aval laissent penser à un possible piégeage minéral du carbone au-delà des limites géométriques relativement réduites du système modélisé.

Abstract* — *Improvement of the Calculation Accuracy of Acid Gas Solubility in Deep Reservoir Brines: Application to the Geological Storage of CO_2 — *The assessment of the short and long term consequences of CO_2 injection in aquifers requires both laboratory experiments and numerical modelling in order to better understand the various physical-chemical processes taking place. Modelling injection in a reservoir, where relatively high temperature (above 50°C), high pressure (several hundreds of bars), and high salinity (greater than that of seawater) conditions are likely to be encountered, thus requires numerical tools able to take into account the specific effects of the various electrolytes dissolved in brines, and the non-ideal behaviour of the CO_2 gaseous phase. This study evaluates the consistency of the various corrections (activity, fugacity, influence of pressure on thermodynamic constants) to be taken into account in geochemical models to meet these calculation accuracy requirements. These corrections were implemented in the thermo-kinetic modelling software SCALE2000 (Azaroual* et al.*, 2004a) which was used to check their validity by comparing the calculation results with available experimental observations and other results from CO_2 solubility calculation models. An estimation of the relative weight of each of the corrections for a 237 g·l^{-1} brine (60°C, pCO_2 = 200 bar) showed a systematic overestimation (higher than 100%) of CO_2 solubility when either salinity (NaCl equivalent) is neglected or gas is considered ideal. The error induced by the NaCl-equivalent approximation compared to real brine is lower (less than 5%).*

The second part of this study presents an application example of a hypothetical scenario of massive CO_2 injection in a carbonated reservoir; data used for the brine composition are actual data (Moldovanyi and Walter, 1992) from the Smackover site (Arkansas, United States). The simulations performed considering a representative elementary volume of saturated bulk rock (porous mineral assemblage saturated with the Smackover brine) with a prescribed constant CO_2 pressure of 150 bar, show two distinctively different behaviours whether the system is assumed to be a closed (batch reactor) or an open reactor fed by a constant brine flow rate. In the first case, the calculations performed with SCALE2000 lead to negligible variations in the mineralogy. In the second case, more representative of the dynamical nature of an injection system, the results show major modifications in the mineralogy finally leading to a strong increase in porosity (from 20% initially to 85% after 50 y of simulated time).

Further calculations were carried out with SCALE2000, now considering a 1D system constituted of a set of four homogeneous identical reactors connected in series (fluid velocity of 1 m.day^{-1}). With initial and boundary conditions similar to those considered earlier, and prescribing a constant pCO_2 in the first reactor only, the results showed that significant dolomite precipitation occurred in the most-downstream reactor hence inducing some CO_2 precipitation. Mass balance calculations performed on the four reactors system finally demonstrated a global loss in total mineral carbon with respect to the amounts initially available. However, the evolution trends observed in the most-downstream two reactors indicated that possible trapping might be expected beyond the relatively limited geometrical boundaries considered in the modelled system.

TABLE OF SYMBOLS

a_{H+}	H^+ activity term, dimensionless
$a_{i,aq}$	activity of the species *i* in the aqueous phase, dimensionless
$a_{i,gas}$	activity of the species *i* in the gaseous phase, dimensionless
f_i	fugacity of gas *i*, Pa
fr	fraction of the total surface area effectively reactive, dimensionless
I	ionic strength, mol·(kg H_2O)$^{-1}$
k	kinetic constant, mol·m^{-2}·s^{-1}
K	thermodynamic equilibrium constant, dimensionless
$m_{i,aq}$	molality of the aqueous species *i*, mol·(kg H_2O)$^{-1}$
P	total pressure, Pa
p_i	partial pressure of gas *i*, Pa
pCO_2	CO_2 partial pressure, Pa
Q	ionic activity product, dimensionless
R	universal gas constant, J·K^{-1}·mol^{-1}
S	total surface area, m^2
T	temperature, K
TDS	Total Dissolved Solids, kg·m^{-3}
V_{net}	effective reaction rate, mol·s^{-1}
$x_{i,gas}$	molar fraction of the species *i* in the gaseous phase, dimensionless
$\Delta\overline{k_r^0}$	partial molal compressibility variation for species involved in a reaction *r*, m^3·mol^{-1}·Pa^{-1}
$\Delta\overline{V_r^0}$	partial molal volume variation for species involved in a reaction *r*, m^3·mol^{-1}
$\Phi_{i,gas}$	fugacity coefficient for the species *i*, dimensionless
$\gamma_{i,aq}$	activity coefficient of the species *i* in the aqueous phase, dimensionless.

INTRODUCTION

CO_2 sequestration in deep saline aquifers emerges as a viable option to mitigate greenhouse gas emissions. Saline aquifers, oil and geothermal reservoirs are the most interesting targets for sequestration. Results of several experimental (*e.g.* Tackenouchi and Kennedy, 1964; Rumpf and Maurer, 1993; Kaszuba *et al.*, 2003; Azaroual *et al.*, 2004b) or modelling (*e.g.* Gunter *et al.*, 1997; Czernichowski *et al.*, 2001; Xu *et al.*, 2004; Gauss *et al.*, 2005) studies have been published. However, knowledge on reactivity and geochemical evolution of such CO_2 enriched systems still has to be improved. Hence, the assessment of the short and long term consequences of injection requires further laboratory experiments and numerical modelling work in order to understand the key processes taking place when CO_2 is injected in a geological reservoir.

High temperature (50°C and above), high pressure (several hundreds of bar), and high salinity (greater than that of seawater) conditions in which CO_2 is likely to be injected, make numerical investigations intricate as, in particular, it is necessary to take into account the non ideal behaviour of both the mixed electrolytes dissolved in brines and the CO_2 gaseous phase.

This study aims at evaluating the impact of the various corrections for aqueous and gaseous phases (activity, fugacity, influence of pressure on thermodynamic constants) to be considered in geochemical models when attempting to calculate CO_2 solubility accurately in brines at high pressure and high temperature. These corrections were implemented in the thermokinetic modelling software SCALE2000 (Azaroual *et al.*, 2004a). After a brief presentation of the theoretical aspects of the Pitzer's formalism, on which these corrections mainly rely, the first part of this paper is devoted to a comparison between modelling results obtained with SCALE2000 and PHREEQC (Parkhurst and Appelo, 1999), and available experimental data from the literature. On the basis of this comparison, we finally propose a quantification of the relative error induced by neglecting each of the suggested corrections. The second part of this article describes an application example of this new version of SCALE2000 to a hypothetical scenario of CO_2 injection in a saline carbonated aquifer (based on actual brine composition data from the Smackover formation, United States). This example focuses particularly on the calculation of CO_2 solubility in the aqueous phase and on the evolution of mineral assemblage under the effect of high CO_2 partial pressure (150 bar).

1 CO_2 SOLUBILITY IN BRINES AT HIGH TEMPERATURE AND PRESSURE

1.1 Gas-Brine Thermodynamic Equilibrium

A reliable assessment of gas solubility has to take into account the complex thermodynamics of the gas-brine-minerals system. Gas solubility is dependent on temperature, pressure, and detailed chemical composition of both the gas and the brine. Considering a species *i* likely to exist in both the gaseous and the aqueous phases, its activity in the aqueous phase ($a_{i,aq}$) is related to its activity in the gaseous phase ($a_{i,gas}$) according to the general law of mass action equation:

$$\frac{a_{i,aq}}{a_{i,gas}} = K_i(P,T) \tag{1}$$

where K_i is the thermodynamic equilibrium constant of the reaction $i_{aq} \leftrightarrow i_{gas}$, *P* is the pressure (bar), and *T* is the absolute temperature (K).

Considering a mixture of ideal gases, the activity of *i* is defined as:

$$a_{i,gas} = \frac{p_i}{p_0} \tag{2}$$

where p_i is the partial pressure of i and p_0 is a reference pressure chosen to be equal to 1 bar.

In the case of real gases, fugacity (f_i in bar) has to be considered instead of partial pressure, so that activity can be written as:

$$a_{i,gas} = \frac{f_i}{p_0} \tag{3}$$

Fugacity is a function depending on the pressure, the temperature, and the molar fraction of the considered species i in the gaseous phase, according to the following equation:

$$f_{i,gas} = x_{i,gas} \cdot P \cdot \Phi_{i,gas}\left(P, T, x_{j \neq i,gas}\right) \tag{4}$$

where $\Phi_{i,gas}$, $x_{i,gas}$, and $x_{j\neq i,gas}$ are, respectively, the fugacity coefficient (dimensionless), the molar fraction (dimensionless) of the species i in the gaseous phase, and the molar fraction of each of the other species j present in the gaseous phase.

Similarly, the activity of an aqueous species depends on the pressure, the temperature, and the solution composition. Although the solution composition effect can be treated as a whole for solutions having a salinity lower than that of sea water ($\approx 35\ g \cdot l^{-1}$), the brines that are typically targeted for acid gas sequestration generally require a differentiation of the specific effect of individual chemical components according to the general equation:

$$a_{i,aq} = \frac{m_{i,aq}}{m_0} \cdot \gamma_{i,aq}\left(P, T, m_{j \neq i,aq}\right) \tag{5}$$

where $\gamma_{i,aq}$, $m_{i,aq}$, and $m_{j\neq i,aq}$ are, respectively, the activity coefficient (dimensionless), the molality ($mol \cdot (kg\ H_2O)^{-1}$) of the aqueous species i in the aqueous phase, and the molality of each of the other aqueous species j; m_0 is a reference molality chosen to be equal to 1 $mol \cdot (kg\ H_2O)^{-1}$.

Combining Equations (1, 3, 4 and 5) leads to the following general formulation of gas solubility in a complex brine:

$$m_{i,aq} = \frac{m_0 K_i \Phi_{i,gas} x_{i,gas} P}{p_0 \gamma_{i,aq}} \tag{6}$$

When pressure and concentration are expressed in bar and in $mol \cdot (kg\ H_2O)^{-1}$ respectively, Equation (6) can finally be simplified as:

$$m_{i,aq} = \frac{K_i \Phi_{i,gas} x_{i,gas} P}{\gamma_{i,aq}} \tag{7}$$

1.2 Activity Correction

Estimating the activity of aqueous species requires the calculation of their activity coefficient integrating the effect of salinity, temperature, and pressure. For low salinity solutions, activity coefficients can be easily calculated by ion association approaches such as Debye-Hückel's, B-Dot, or Davies'. These approaches, implemented in most of the geochemical codes such as PHREEQC (Parkhurst and Appelo, 1999) or EQ3/6 (Wolery, 1992), are mathematically simple and well parameterised (Helgeson *et al.*, 1981).

However, for higher salinities, the calculated results diverge from observations, even in the case of NaCl solutions *(see Fig. 1)*. In these cases, the use of a more specific interaction model such as Pitzer's model (Pitzer, 1973) is necessary. Pitzer's model, implemented in SCALE2000 (Azaroual *et al.*, 2004a), has been specifically designed to reproduce experimental data at high ionic strength.

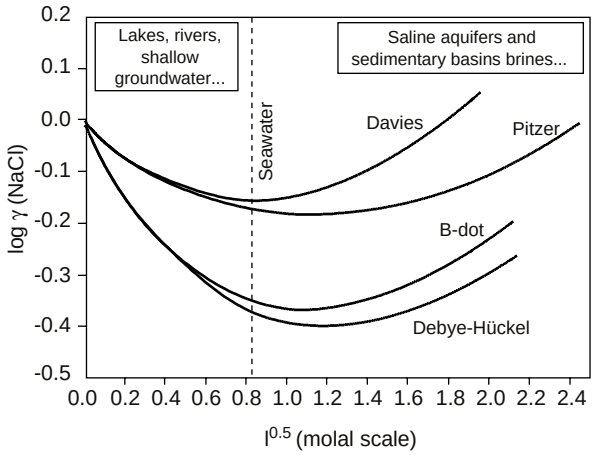

Figure 1

Mean activity coefficient for NaCl (γNaCl) *vs.* ionic strength of the solution, calculated at 25°C, 1 bar, using various activity models.

Compared to ion association models, Pitzer's formalism is mathematically more complex and relies on many parameters. Despite the lack of some of experimental data, notably for complex electrolytic solutions at high temperature, it was finally possible to build a consistent Pitzer's database based on a very systematic and refined interpolation, extrapolation, and verification work using the simple electrolytes data available from the literature. Hence, in its actual version, the model accurately describes the behaviour of carbonate-gas-water systems for temperature and pressure conditions ranging respectively from 25 to 250°C and 1 to 1000 bar, and for high salinity solutions (ionic strength up to about 6 M) in the system Na-K-Ca-Mg-Sr-Ba-Fe-Cl-SO_4-HS-OH-H-Ac-CO_3-HCO_3-H_2S-CO_2-AcH-SiO_2-H_2O. The geochemical software SCALE2000 (Azaroual *et al.*, 2004a) relies on this Pitzer's formulation and relevant databases. SCALE2000 was validated against numerous experimental data available in the literature (Azaroual *et al.*, 2004c).

Figure 1 presents calculation results of NaCl activity coefficient as a function of the squared root of the ionic

strength I (molal) for a pure NaCl solution at 25°C and 1 bar. At a salinity beyond that of seawater (ionic strength of approximately 0.7), this figure clearly shows significant discrepancies between the results obtained with SCALE2000, relying on Pitzer's formulation, and those based on simple ion association approaches (Debye-Hückel, Davies, B-Dot). Considering that Pitzer's formulation is the most adequate for problems involving high salinity solutions (Harvie *et al.*, 1984) as confirmed by experimental measurements, it can be concluded that Davies' formalism is not reliable for thermodynamic predictions for solutions more saline than seawater. Figure 1 also confirms that the Debye-Hückel formalism can only be applied at much lower ionic strengths than the Davies formalism, which practically makes it unusable for brackish and saline natural systems.

1.3 Thermodynamic Equilibrium Constant

The accuracy of the thermodynamic equilibrium constants is of course of major importance to estimate an actual gas or mineral solubility in a complex system. Geochemical codes (EQ3/6, PHREEQC, etc.) generally only take into account the influence of the temperature on equilibrium constants, thereby neglecting the pressure effect, which is usually assumed to be less significant (Kharaka *et al.*, 1988). However, in CO_2 geological sequestration problems, the pressure involved may reach several hundreds of bars, and in this case, its effect on equilibrium constants becomes significant. A first formulation proposed by Monnin (1990) for calculating the influence of the pressure on equilibrium constants (valid for pressures lower than 1000 bar) can be used:

$$\ln(K(T,P)) = \ln(K(T,P_0)) - \frac{(P-P_0)\Delta\overline{V_r^0}(T,P_0)}{RT} + \frac{(P-P_0)^2\Delta\overline{k_r^0}(T,P_0)}{2RT} \quad (8)$$

where T, P, and R are, respectively, the temperature, the pressure, and the universal gas constant; index 0 refers to a reference state, and $\Delta\overline{V_r^0}$ and $\Delta\overline{k_r^0}$ stand respectively for partial molal volume and partial molal compressibility variations for the components involved in a reaction r. This approach assumes that $\Delta\overline{V_r^0}$ and $\Delta\overline{k_r^0}$ do not depend on pressure but it has been shown that these functions might however vary significantly with pressure (Johnson *et al.*, 1992). A more powerful formalism with a more extended validity domain ($0 < T < 1000$°C; $1 < P < 5000$ bar), explicitly taking into account the pressure effect on $\Delta\overline{V_r^0}$ and $\Delta\overline{k_r^0}$, was developed by Johnson *et al.* (1992). In order to improve the accuracy of the model results, this latter formalism was finally implemented in SCALE2000.

Figure 2 illustrates this pressure effect for the reaction $CO_{2,aq} \leftrightarrow CO_{2,gas}$. It is interesting to notice that the slope of the curves increases with temperature. Thus, considering the temperature domain relevant for CO_2 geological sequestration, this result highlights the increased inaccuracy when this pressure effect is not accounted for in the models.

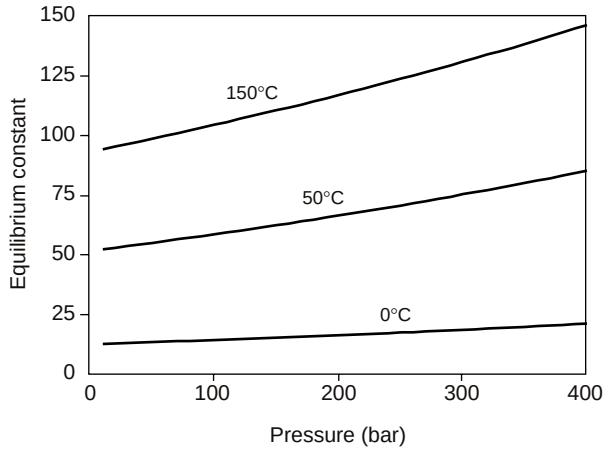

Figure 2

Influence of pressure on the thermodynamic equilibrium constant of the reaction $CO_{2,aq} \leftrightarrow CO_{2,gas}$.

1.4 Fugacity Correction

The calculation of gas fugacity necessitates first to evaluate the molal volume which depends on the gas phase composition, the pressure, and the temperature. Among the various equations of state (EOS) available in the literature, those from Duan *et al.* (1992a, 1992b, 2003) appeared to be well adapted to the problem of acid gas sequestration as they asses phase changes occurring in the pressure-temperature domain considered. The general form of these equations, derived from those of Lee and Kesler (1975), can be found in Duan *et al.* (1992b, Equations (1, 9); Table 1 and 2). They permit to calculate the molar volume of a pure or mixed gas phase as well as the fugacity coefficient of each gas.

Duan *et al.*'s formalism was implemented in version 3.1 of SCALE2000. Figure 3 presents a 2D graph of the calculated CO_2 fugacity coefficient as a function of pressure and temperature. Also represented on Figure 3 is the critical point of CO_2. It can be observed that in gaseous and supercritical phases, CO_2 fugacity coefficient ranges from 0.3 to 1. For example, under conditions typical for CO_2 sequestration, *i.e.* 200 bar and 60°C, the fugacity coefficient for pure CO_2 will be 0.45, leading to a fugacity value of 90 bar instead of 200 bar of assumed partial pressure of CO_2 without applying any correction (thus assuming a fugacity coefficient of 1).

Figure 4 shows a good agreement between SCALE2000 calculation results and experimental measurements of CO_2 solubility in pure water for a pressure up to 400 bar and a temperature up to 250°C, confirming the validity of the fugacity coefficient and equilibrium constant calculations.

TABLE 1

Chemical composition of the reference waters considered in the simulations. **A**: initial analytical data from the Smackover formation water (fluid sample no. 71 in Moldovanyi and Walter, 1992). **P1**: initial speciation calculated with PHREEQC at 25°C. **S1**: initial speciation calculated with SCALE2000 at 25°C. **P2**: initial speciation calculated with PHREEQC at the reservoir temperature (71°C). **S2**: initial speciation calculated with SCALE2000 at the reservoir temperature (71°C). **S3**: speciation calculated with SCALE2000 at the reservoir temperature (71°C) assuming equilibrium with calcite. **S4**: speciation calculated with SCALE2000 at the reservoir temperature (71°C) assuming equilibrium with the hypothesised mineralogical composition of the reservoir (anhydrite, calcite, dolomite, quartz, siderite). **P3**: speciation calculated with PHREEQC at the reservoir temperature (71°C) assuming equilibrium with pCO_2 = 150 bar. **S5**: speciation calculated with SCALE2000 at the reservoir temperature (71°C) assuming equilibrium with pCO_2 = 150 bar (calculated fugacity = 79.8 bar). **P4**: speciation calculated with PHREEQC at the reservoir temperature (71°C) assuming equilibrium with pCO_2 = 79.8 bar (CO_2 fugacity value calculated by SCALE2000).

	A	**P1**	**S1**	**P2**	**S2**	**S3**	**S4**	**P3**	**S5**	**P4**
Temperature (°C)	25	25	25	71	71	71	71	71	71	71
Pressure (bar)	1	–	1	–	180	180	180	–	180	–
Density ($kg \cdot l^{-1}$)	1.132	–	1.134	–	1.107	1.107	1.108	–	1.107	–
pH	6.30(*)	6.34	6.86	6.27	6.53	5.59	5.55	2.95	3.46	3.16
Total alkalinity ($meq \cdot (kg\ H_2O)^{-1}$)	3.90	–	3.89	3.90	3.89	1.71	1.65	3.90	3.93	3.90
CO_2 fugacity (bar)	–	0.0162	0.0113	0.0389	0.0507	0.199	0.203	150	79.8	79.8
Composition ($mmol.(kg\ H_2O)^{-1}$)										
C	3.69	3.69	3.68	3.69	3.68	2.59	2.56	1407.00	461.49	750.90
Cl	3620.36	3566.00	3583.73	3566.00	3583.73	3583.67	3583.67	3566.00	3583.78	3566.00
Br	29.52	29.51	(**)	29.51	(**)	(**)	(**)	29.51	(**)	29.51
B	5.34	5.34	–	5.34	–	–	–	5.34	–	5.34
F	0.56	0.56	–	0.56	–	–	–	0.56	–	0.56
I	0.20	0.20	–	0.20	–	–	–	0.20	–	0.20
SO_4	4.73	4.73	4.72	4.73	4.72	4.72	7.42	4.73	4.73	4.73
Na	2403.17	2403.00	2396.83	2403.00	2396.83	2396.79	2396.79	2403.00	2396.87	2403.00
K	15.31	15.31	15.27	15.31	15.27	15.27	15.27	15.31	15.27	15.31
Li	3.23	3.23	(**)	3.23	(**)	(**)	(**)	3.23	(**)	3.23
Ca	475.51	475.40	474.24	475.40	474.24	473.14	557.28	475.50	474.24	475.40
Mg	109.18	109.20	108.89	109.20	108.89	108.89	23.54	109.20	108.89	109.20
Sr	8.93	8.93	8.91	8.93	8.91	8.91	8.91	8.93	8.91	8.93
SiO_2	0.50	0.50	0.50	0.50	0.50	0.50	0.24	0.50	0.50	0.50
Fe	0.44	0.44	0.44	0.44	0.44	0.44	4.32	0.44	0.44	0.44
Acetate	0.27	0.27	0.27	0.27	0.27	0.27	0.27	0.27	0.27	0.27
Saturation index										
Anhydrite	–	–0.47	–0.36	–0.09	–0.23	–0.23	0	–0.09	–0.18	–0.09
Calcite	–	0.42	1.21	0.99	1.28	0	0	–2.09	–1.59	–1.93
Dolomite	–	1.29	3.02	2.56	3.29	0.73	0	–3.59	–2.43	–3.28
Quartz	–	0.94	1.03	0.24	0.32	0.32	0	0.26	0.32	0.26
Siderite	–	–0.95	0.13	–0.54	0.36	–0.92	0	–3.62	–2.59	–3.46

* Measured at the reservoir temperature (71°C).
** Chemical element not considered for speciation calculation but taken into account for density calculation.

Figure 5 also shows a satisfactory agreement between calculated CO_2 solubility and experimental measurements in NaCl, $CaCl_2$, and $MgCl_2$ solutions for electrolyte concentrations as high as 5 molal at 1 bar and 25°C, corroborating the validity of the activity coefficient calculation at standard conditions. Another important aspect pointed out by the results of Figure 5 is the great variability of CO_2 solubility according to the nature of the electrolyte. Hence, the detailed knowledge of the chemical composition of the brine appears to be a key point in any evaluation of the CO_2 sequestration capacity of a potential site.

In order to evaluate the accuracy of the model at high temperature, we performed a series of calculations for a 1 M NaCl solution at 150°C for pressures ranging from 50 to 400 bar. The calculation results presented on Figure 6 can be favourably compared to the measurements of Takenouchi and Kennedy (1964). On the basis of the experimental data from Malinin and Kurovskaya (1975), we carried out other CO_2 solubility calculations in 0.44 M and 0.88 M $CaCl_2$ solutions for moderate temperatures (25 to 75°C). The calculation results are also in very good agreement with the measurements *(Fig. 7)*.

TABLE 2

Major parameters relative to mineral properties used in *batch* and open-reactor simulations. Initial concentrations were calculated assuming a water-rock ratio of 1:4 in volume (20% porosity). Last five columns refer to parameters used in Equations (9) and (10). Specific surfaces were estimated based on a classical spherical grain approach.

	Initial weight (%)	**Molal mass** ($g \cdot mol^{-1}$)	**Molal volume** ($cm^3 \cdot mol^{-1}$)	**Initial volume** (%)	**Initial concentration** ($mol \cdot l^{-1}$)	**Reference temperature** (K)	**log *k(Tr)***	**Activation energy** ($J \cdot mol^{-1}$)	**Specific surface** ($cm^2 \cdot mol^{-1}$)	**Precipitation surface** (cm^2)
Dolomite	70	184.401	64.365	70.04	43.53	298.15	–12.0	40,000	19309.5	10^5
Calcite	12	100.087	36.934	12.69	13.75	298.15	–11.0	41,850	11080.2	10^5
Anhydrite	10	136.142	45.94	9.67	8.42	523.15	–9.6576	41,850	13782	10^4
Quartz	5	60.084	22.688	5.41	9.54	298.15	–17.38	76,600	6806.4	10^3
Siderite	3	115.856	29.378	2.18	2.97	298.15	–12.0	40,000	8813.4	10^4

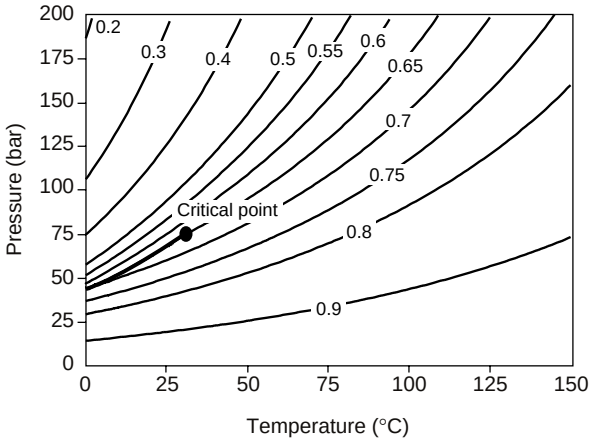

Figure 3

Pure CO_2 fugacity coefficient calculated with SCALE2000 as a function of the pressure and the temperature.

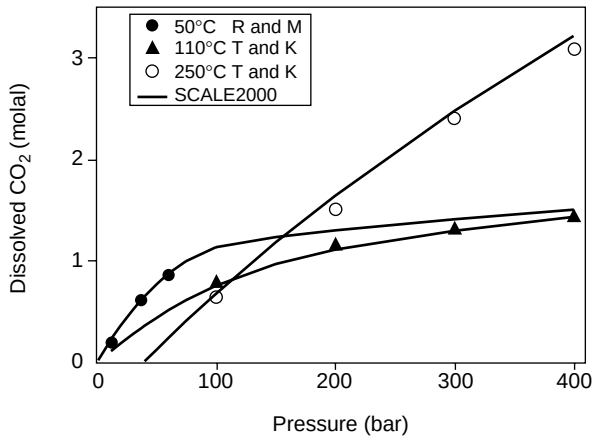

Figure 4

CO_2 solubility in pure water calculated with SCALE2000 compared to the experimental measurements of Takenouchi and Kennedy (1964) (*T* and *K*), and Rumpf and Maurer (1993), (R and M).

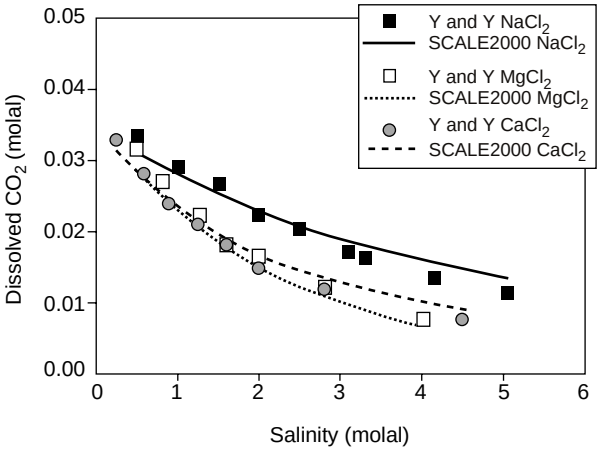

Figure 5

CO_2 solubility in NaCl, $CaCl_2$, and $MgCl_2$ solutions (1 bar and 25°C) calculated with SCALE2000 compared to the experimental measurements of Yasunichi and Yoshida (1979), (Y and Y).

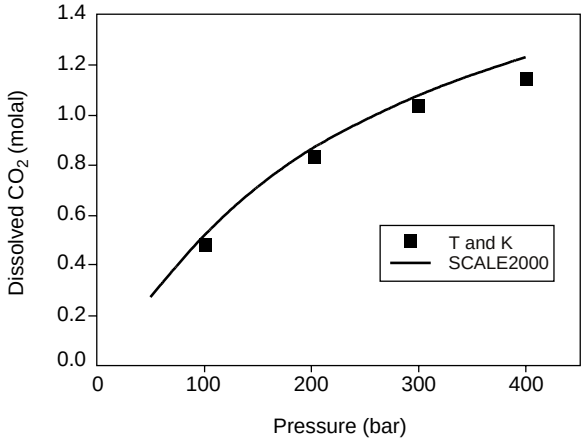

Figure 6

CO_2 solubility in a 1 M NaCl solution at 150°C *vs.* pressure. Results calculated with SCALE2000 are compared to the experimental measurements of Takenouchi and Kennedy (1964), (T and K).

Because of the scarcity of CO_2 solubility data for electrolyte systems other than NaCl, especially at high temperatures, we were not able to do any further validation analysis. However, the results achieved up to now lead us to believe that all the corrections implemented in SCALE2000 notably improve CO_2 solubility prediction.

Figures 4 to 7 finally highlight the importance of taking into account the effects of the temperature, the pressure, and the fugacity as well as the necessity to consider the specificity of the electrolyte when calculating CO_2 solubility, particularly in the context of geological sequestration where relatively high pressure (several hundreds of bar), temperature (above 50°C) and salinity (higher than that of seawater) conditions are likely to be encountered.

1.5 Relative Weight of the Various Corrections

As an illustration of the relative weight of the different corrections accounted for in SCALE2000 (*i.e.* fugacity, effect of the pressure on equilibrium constants, activity model), we performed CO_2 solubility calculations using PHREEQC (Parkhurst and Appelo, 1999) without any fugacity nor activity correction, PHREEQC with the fugacity coefficient corrected "by hand" (on the basis of the value calculated by SCALE2000), and SCALE2000 taking into account all the corrections. These calculations were applied to a 1 M NaCl solution at 150°C and for pressure varying from 50 to 400 bar. The PHREEQC input file used for these calculations is provided in Appendix 1.

The graphs represented on Figure 8 show a good agreement between the results of the calculations performed with SCALE2000 and the experimental measurements over the whole pressure range. In contrast, important discrepancies between experimental and PHREEQC results (11% at 50 bar, 127% at 400 bar) are observed. The fugacity correction notably reduces the error but the discrepancy still remains noticeable (4% at 50 bar, 47% at 400 bar). Consequently, these results prove that the main error arises from neglecting the fugacity correction. However, neglecting the pressure effect on the equilibrium constants as well as considering an inadequate activity model also contribute significantly to the inaccuracy of the CO_2 solubility calculations.

In an attempt to quantify the impact of the aqueous activity model on the estimated CO_2 solubility, we performed the following series of calculations: on one hand we considered the detailed composition of the brines and, on the other hand, an equivalent-NaCl solution expressed as total dissolved solids (TDS). The equivalent-NaCl solution is a classical approach used in many solubility calculations aiming to simulate the salting out effect (Drummond, 1981). The simulation conditions were 200 bar and 60°C and the 35 brine compositions considered were selected among data from Hitchon *et al.* (1971), Langmuir and Melchior (1985), Kelly *et al.* (1986), Leach *et al.* (1991), Land (1995), Stueber *et al.* (1998), Demir and Seyler (1999), and Martel *et al.* (2001). The results presented on Figure 9a globally show relatively small gaps between the two calculation methods even though a significant gap can be observed for the highest salinity. The same results, plotted in terms of relative variation between the two calculation methods *(Fig. 9b)*, confirm that the error induced by the equivalent-NaCl approximation has a relatively low impact on the dissolved CO_2 value (less than 5%) for the brines considered in our simulations. The maximum discrepancy on Figure 9b (above 15%) is observed for a high-TDS brine containing a majority

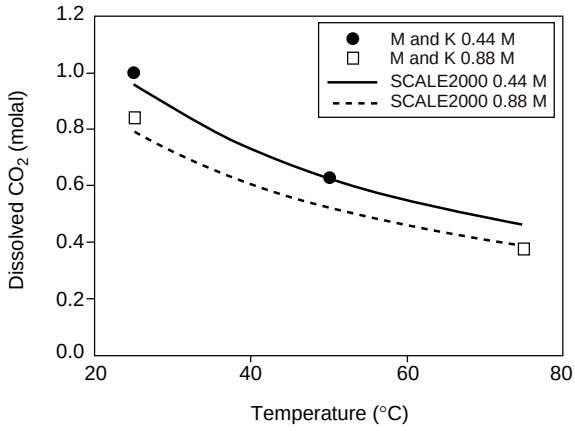

Figure 7

CO_2 solubility in $CaCl_2$ solutions at 48 bar *vs.* temperature. Results calculated with SCALE2000 are compared to the experimental measurements of Malinin and Kurovskay (1975), (M and K).

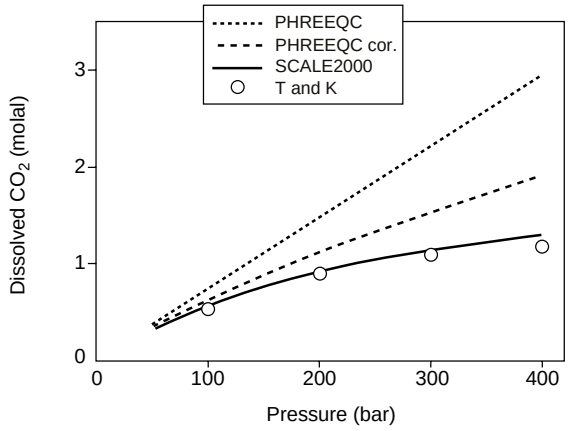

Figure 8

Comparison between CO_2 solubility value (150°C in a 1 M NaCl solution) calculated with 1) PHREEQC, 2) PHREEQC with fugacity correction, 3) SCALE2000, and experimental data of Takenouchi and Kennedy (1964), (T and K).

of calcium (Kelly *et al.*, 1986). This observation suggests that the small differences observed on Figure 9b are probably due to the fact that the majority of the brines were of NaCl type.

However, a second comparison now performed with equivalent-NaCl solutions of the same ionic strength (thus including the ions charge inpact), shows that the approximated method systematically underestimates CO_2 solubility *(Fig. 10a)*. The relative error induced by NaCl approximation *(Fig. 10b)* becomes significant for the majority of the brines (between 5% and 20%).

Consequently, these results show that the use of a simplified equivalent-NaCl approach may be acceptable only for NaCl-type waters of relatively low salinity. In the general case, the use of models accounting for the complete composition of the brine appears to be suitable. When not considering this correction, the error generated may reach significant values beyond the acceptable limit of 5%.

Our attempt of quantification of the relative weight of all the corrections described above is summarised in Figure 11. We arbitrary chose to work on a 237 g·l^{-1} brine at 200 bar

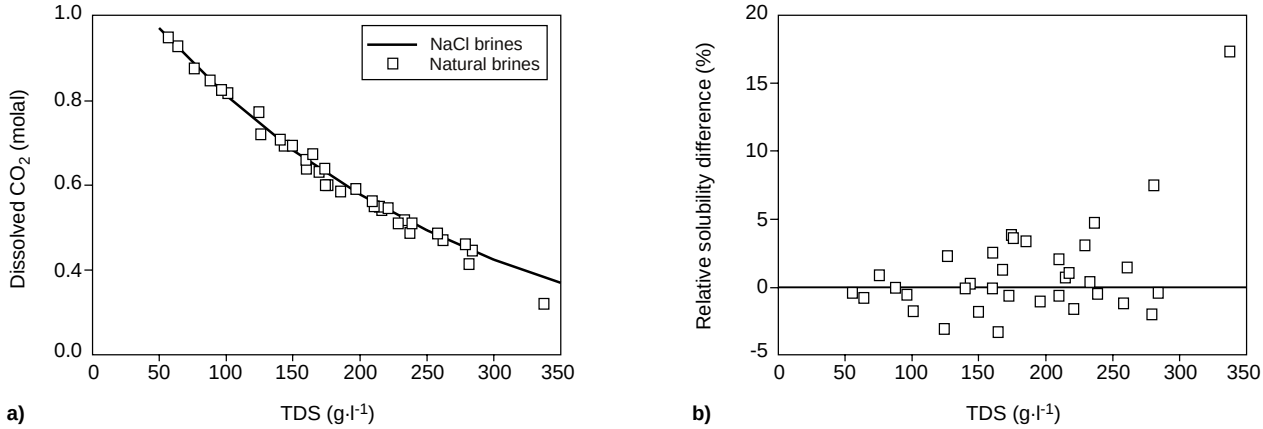

Figure 9

a) calculated amounts of dissolved CO_2 (200 bar, 60°C) for natural brines and for NaCl-equivalent solutions *vs.* salinity (TDS). Composition data from Hitchon *et al.* (1971): Na-Ca-(Mg)-Cl, 124-278 g·l^{-1}; Langmuir and Melchior (1985): Na-(Ca-Mg)-Cl, 140-221 g·l^{-1}; Kelly *et al.* (1986): Ca-Na-Cl, 184-337 g·l^{-1}; leach *et al.* (1991): Na-Cl, 261 g·l^{-1}; Land (1995): Ca-Na-Cl and Na-Ca-Cl, 88-172 g·l^{-1}; Stueber *et al.* (1998): Na-Ca-Cl, 101-215 g·l^{-1}; Demir and Seyler (1999): Na-Ca-Cl, 126 g.l^{-1}; Martel *et al.* (2001): Na-Ca-Cl, 58-177 g·l^{-1}. b) relative variation (%)* *vs.* salinity (TDS) in CO_2 solubility calculated for NaCl-equivalent solutions with respect to solubility calculated for natural brines.

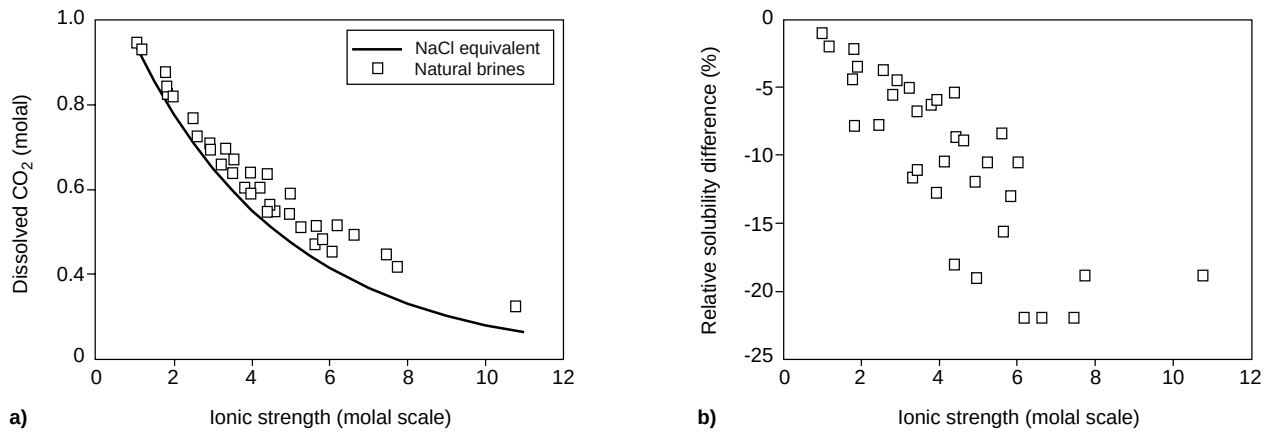

Figure 10

a) calculated amounts of dissolved CO_2 (200 bar, 60°C) for natural brines and NaCl-equivalent solutions *vs.* ionic strength. Chemical compositions are identical to those of Figure 9. b) relative variation (%)* *vs.* ionic strength in CO_2 solubility calculated for NaCl-equivalent solutions with respect to solubility calculated for natural brines.

(*) Relative solubility difference (%) = $100 \cdot \left(\frac{m_{\text{NaCl equivalent}} - m_{\text{Natural brine}}}{m_{\text{Natural brine}}} \right)$.

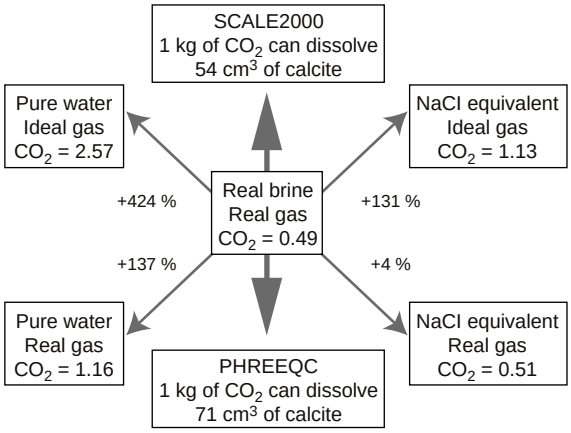

Figure 11

Synthesis diagram of the relative weights of the various corrections applied to the calculation of CO_2 solubility and mineral equilibrium for a 237 g·l^{-1} brine at 60°C and 200 bar. Indicated percentages are calculated with respect to the reference water composition "real brine, real gas". Quantity of dissolved CO_2 is expressed in mol·(kg H_2O)$^{-1}$.

and 60°C. Under these calculation conditions, with CO_2 treated as a real gas (fugacity coefficient of 0.45) assumed to occupy the whole gaseous phase, and taking into account the real brine composition (with all activity corrections), finally led to a CO_2 solubility of 0.49 mol·(kg H_2O)$^{-1}$. Assimilating CO_2 to an ideal gas and neglecting salinity (thus considering pure water) induces an error on CO_2 solubility which is more than 400%! Figure 11 also shows that considering either salinity (NaCl equivalent) or non-ideality of CO_2 (applying fugacity correction) notably improves the prediction even though the calculated solubility remains largely over-estimated (more than 100%). These results highlight the necessity to take into account both the fugacity correction and the salinity effect in order to get good estimates of CO_2 solubility. In comparison, the improvement provided by considering the real brine composition instead of its NaCl-equivalent remains relatively small in this case (less than 5%). With this dissolved CO_2 reference value of 49 mol·(kg H_2O)$^{-1}$, the results on calcite solubility underline the impact of the aqueous activity model used: we calculated that 1 kg of dissolved CO_2 in the brine could lead to the dissolution of 71 cm^3 of calcite or 54 cm^3 of calcite using, respectively, PHREEQC or SCALE2000.

The percentages indicated in Figure 11, though to be considered as exact only for the specific brine considered in the simulations, however represent good indicators of the relative impact of each of the corrections when considered separately. When all the corrections were simultaneously taken into account (calculations using SCALE2000), the results obtained could always be favourably compared to available experimental measurements, thus indicating that the improvement in the prediction was significant.

2 EXAMPLE OF APPLICATION TO CO_2 SEQUESTRATION

In order to illustrate the improvements provided by the integration of fugacity and activity corrections in the simulation of gas-brine-minerals mass exchange processes, we studied the potential effects of CO_2 injection in a deep brine reservoir typical of some of those targeted for CO_2 geological sequestration. We considered here a hypothetical scenario of CO_2 injection in a Smackover-type formation (Arkansas, United State) for which detailed brine composition data were available in Moldovanyi and Walters (1992). The Smackover site is mainly characterised by a carbonate-evaporite formation, fluid temperatures ranging from 51 to 105°C, *in situ* pressure of 150 to 400 bar, Na-Ca-Cl brines with TDS varying from 152 to 342 g·l^{-1} (Moldovanyi and Walters, 1992). For this study, we selected a 196 g·l^{-1} brine (sample no. 74 of Tables 1 to 3 in Moldovanyi and Walters, 1992) that was collected from a well located in the northern reservoir, at a depth of 1715 m and at a bottom hole temperature of 71°C. Its detailed chemical composition is given in Table 1 (column "A"). For the water-rock interaction simulations, we considered a hypothetical mineralogical composition (in weight: dolomite, 70%; calcite, 12%; anhydrite, 10%; quartz, 5%; siderite, 3%) consistent with carbonated reservoir conditions. For the following calculations, we assumed constant *in situ* pressure and temperature conditions of 180 bar and 71°C. Laboratory pressure and temperature conditions were supposed to be 1 bar and 25°C.

2.1 Initial Speciation Calculations

Simulating a massive CO_2 injection scenario first requires the definition of an initial reference state that we chose to be thermodynamic equilibrium between the brine and the mineralogical assemblage defined above. Prior to that simulation, it is then necessary to calculate the formation water speciation on the basis of the analysis data, in order to check the consistency between the analytical results (with inevitable measurement inaccuracies, electric charge imbalance, etc.) and the thermodynamic model results. These initial calculations were carried out with both SCALE2000 and PHREEQC to allow for comparison and the results are presented in details in Table 1. It has to be noticed that all the data presented in Table 1 (except temperature, pressure and most of the data in column "A" which are actually used as input in the models) are calculation results. Moldovanyi and Walters (1992) indicated however that their pH analyses must be viewed as approximations because of the potential for CO_2 degassing from brine samples. Consequently, we did not use the pH value as an input data in the input files (see Appendix 2 for the PHREEQC input file) and the carbonate system was constrained prescribing the total alkalinity

(equivalent to *At* in Moldovanyi and Walters, 1992) and the total dissolved inorganic carbon (equivalent to *TIC* in Moldovanyi and Walters, 1992) that we considered to be more reliable input data (Moldovanyi and Walters describing a more careful analytical protocol for these specific measurements).

The first series of calculations aimed at verifying the global consistency of the input data set. For that purpose, we calculated with SCALE2000 and PHREEQC the brine characteristics at the laboratory conditions. In both codes, electro-neutrality was reached by automatically adjusting the total amount of chloride. The results detailed in Table 1 (columns "P1" and "S1") are both in very good agreement with the analytical data (column "A") in terms of total amounts of chemical elements except for chloride which was obviously slightly modified for electro-neutrality adjustment. This result is not of major interest in itself as the total amounts in column "A" *(Table 1)* were used as input data in the codes; it just confirms the correct behaviour of the models algorithms for converting initial input data in $mg \cdot l^{-1}$ into molalities ($mmol \cdot (kg\ H_2O)^{-1}$). However, it has to be noticed that, contrary to PHREEQC, SCALE2000 did not use the density value (which is a key-parameter in these unit conversion calculations) as an input but recalculated it based on a formalism evaluating the volumetric properties of the aqueous phase using Pitzer's ion interaction approach (Monnin, 1994). It is then interesting to remark the very good agreement between the measured density at 25°C ($1.132\ kg \cdot l^{-1}$) and the density calculated by SCALE2000 ($1.134\ kg \cdot l^{-1}$) considering moreover that some of the trace elements present in the studied sample (B, F, I, Mn, Zn, Br, Li) are not accounted for in SCALE2000 speciation calculations (however, Li and Br initial amounts are taken into account in density calculation). Due to the fact that pH measurement was performed immediately upon collection of the fluid sample (thus at a temperature close to that of the reservoir, *i.e.* 71°C), the values of calculated and measured pH must not be compared directly even though they are very close between PHREEQC results (*Table 1*, column "P1") and analytical data. Lastly, the comparison between PHREEQC and SCALE2000 results (*Table 1*, column "P1" and "S1") show some discrepancies for Saturation Indexes, pH, and CO_2 fugacity; provided that gaps between thermodynamic equilibrium constant used in the two codes are very weak, this can be easily explained by the activity models considered *i.e.* Davies in PHREEQC, and Pitzer in SCALE2000.

In a second step, we performed calculations under reservoir conditions (71°C, 180 bar) using PHREEQC (*Table 1*, column "P2") and SCALE2000 (*Table 1*, column "S2"). It has to be noticed that the pressure effect on equilibrium constants (see *Section 1.3*) is not taken into account in PHREEQC. The pH value of 6.27 calculated with PHREEQC is close to the measured pH (6.30) whereas SCALE2000 predicts a higher pH value (6.53); however, analytical uncertainties on pH measurement previously mentioned do not permit to be conclusive on calculation accuracy, referring to this only pH criteria. However, on the basis of the results obtained with both SCALE2000 and PHREEQC and even though some slight discrepancies were observed with respect to the analytical data, it can be concluded that the calculated brine composition is globally consistent with the very detailed analytical data set provided by Moldovanyi and Walters (1992).

Once this initial water composition was characterised, we performed another speciation calculation with SCALE2000 assuming thermodynamic equilibrium with calcite, which is likely to occur in a carbonated reservoir. The results are presented in Table 1 (column "S3") and it is interesting to notice that, in this case, CO_2 fugacity is notably greater than in the case where calcite equilibrium was not supposed ("S2" water) while pH, alkalinity, and dissolved carbon are lower. These results are consistent with Moldovanyi and Walters' hypothesis of degassing during sampling. The loss in total carbon and calcium is explained by over-saturation of water "S2" with respect to calcite inducing calcite precipitation to reach thermodynamic equilibrium; the slight variations observed in Cl and Na concentrations (main components of the brine), expressed in molalities, are explained by the variation in the total amount of pure water (H_2O) in the brine composition induced by the precipitation reaction.

The next initial calculation performed with SCALE2000 aimed at establishing a reference water composition to be used as an initial condition for the CO_2 injection simulations presented Section 2.2. For that purpose, we equilibrated the "S2" water with the selected mineral assemblage: calcite, dolomite, anhydrite, siderite, and quartz. To reach equilibrium, SCALE2000 predicted precipitation of dolomite and quartz (15.739 and 0.016 $g \cdot (kg\ H_2O)^{-1}$ respectively) and dissolution of anhydrite, siderite, and calcite (0.367, 0.45, and 16.585 $g \cdot (kg\ H_2O)^{-1}$ respectively) leading to significantly different concentrations for the major species involved in the precipitation/dissolution reactions (C, Na, Ca, Mg, Si, Fe in Table 1, column "S4"). Compared to the previous calculation (equilibrium with calcite alone, "S3" water), pH, alkalinity, and total carbon do not vary significantly.

In this particular example where salinity (TDS = $196\ g \cdot l^{-1}$) is more than five times higher than that of seawater, the importance of the activity model accuracy was underlined as calculation results obtained with PHREEQC (Davies activity model) and SCALE2000 (complete Pitzer's ion interaction model), even though comparable in terms of elementary composition, might lead to significant discrepancies when comparing pH, CO_2 fugacity, or saturation indexes. In order to corroborate the results presented in the first section of this article, we have performed a last series of simulations more particularly focusing on the fugacity correction effect. Starting from the initial water composition ("P2" and "S2", for PHREEQC and SCALE2000 calculations, respectively),

we prescribed a high CO_2 pressure of 150 bar (this CO_2 pressure remaining constant for the whole simulation). The speciations obtained are detailed in Table 1 (column "P3" for PHREEQC and "S5" for SCALE2000) and it can be observed that neglecting the fugacity correction leads to an overestimation of the total dissolved carbon of more than 300%! Attempting to reduce this error, we prescribed in the PHREEQC input file (see *Appendix 2*) the CO_2 fugacity value calculated by SALE2000 (79.8 bar) instead of the partial pressure of CO_2 (150 bar); one must remark that, obviously, this fugacity value is generally not available as an input data for all conditions of potential interest. The results presented in Table 1 (column "P4") show that, despite this artificial correction, the error made on the total dissolved carbon still reaches 50%. This demonstrates the importance of the fugacity correction that was implemented in SCALE2000 when attempting to evaluate amounts of dissolved CO_2; moreover, for cases where the salinity of the fluid is above that of seawater (which are likely to be frequently encountered in many CO_2 injection studies), it is also of major importance to take into account in the models the combined effect of salinity, pressure, and temperature.

2.2 Effect of High pCO_2 on the Geochemical System

The CO_2 "injection" simulation first considered a closed reactor (*batch*) with a prescribed initial water-rock ratio of 1 to 4 in volume (namely 1 l of fluid for a total volume of 4 l of minerals) corresponding to the assumed initial porosity of 20%. In this reactor (total pressure: 180 bar; temperature: 71°C), we applied for the whole simulation duration a constant CO_2 partial pressure of 150 bar (leading to a fugacity value of 79.8 bar, according to SCALE2000 calculation). The idea was to estimate on a representative elementary volume of the geochemical system the effects of a high CO_2 pressure likely to be encountered in massive CO_2 sequestration scenarios. These calculations were carried out using the "kinetics" module of SCALE2000 where the incorporated kinetic law for mineral dissolution/precipitation is derived from the Transition State Theory (Lasaga, 1984) for which the effective reaction rate V_{net} (mol·s^{-1}) can be expressed according to the following general equation:

$$V_{net} = k \cdot S \cdot fr \cdot (a_{H^+})^n (1 - \frac{Q}{K}) \qquad (9)$$

where k is a kinetic constant expressed in mol·cm^{-2}·s^{-1}, S is the total surface area (cm^2) assumed to be a constant term when precipitation occurs and proportional to the remaining mineral mass in the case of dissolution, fr is the fraction of the total surface area effectively reactive, a_{H+} is the H^+ activity term, Q is the ionic activity product, and K is the thermodynamic equilibrium constant of the considered precipitation/dissolution reaction. The reactive surface area, which is one of the most difficult parameters to characterise, was defined here on the basis of a classical spherical grain model; in our simulations, fr was set to 1 and no pH effect on kinetic was considered (n set to 0), whatever mineral species is considered. The kinetic constant k is calculated, for each mineral species, in function of the temperature according to the following law (Aagaard and Helgeson, 1982):

$$\log k(T) = \log k(T_r) + \frac{E_a}{R}\left(\frac{1}{T_r} - \frac{1}{T}\right) \qquad (10)$$

In which E_a is the activation energy and T_r is a reference temperature. The main operational parameters for this simulation are presented in Table 2 (initial fluid composition being detailed in Table 1, column "S4").

The main results of this batch simulation are illustrated on Figure 12 where mineral concentration variations are expressed as relative mass variations calculated according to the following equation:

$$\text{Relative mass variation (\%)} = 100 \times \left(\frac{C_{i,\min}(t) - C_{i,\min}(t=0)}{C_{i,\min}(t=0)}\right) \qquad (11)$$

In this equation, $C_{i,\min}(t = 0)$ and $C_{i,\min}(t)$ are, respectively, the initial concentration of mineral i and its concentration at time t, expressed in g·m^{-3} of saturated bulk rock. We preferred this unit of concentration over the "classical" g·(kg H_2O)$^{-1}$ as this latter unit may sometimes be a bit confusing for minerals. For example, considering a rigorously constant number of moles of a mineral (*e.g.*: quartz) in thermodynamic equilibrium with the fluid phase, variation with time of this mineral concentration may however occur if expressed in g·(kgH_2O)$^{-1}$ because of other progressing chemical reactions (*e.g.*: precipitation/dissolution of a hydrated mineral such as gypsum) inducing fluctuations of the H_2O amount in solution. This concentration variation could then be erroneously interpreted as precipitation or dissolution of the non-reactive mineral (quartz in this example).

What can be seen first on Figure 12 is that the response time of the system to this strong initial input in CO_2 is relatively short as within a few tens of days, a new thermodynamic equilibrium state is reached. On the other hand, the mineralogical composition changes only slightly: the relative variations induced by the presence of 0.48 mol·(kg H_2O)$^{-1}$ of dissolved carbon (to be compared to 0.0026 mol·(kg H_2O)$^{-1}$, which is the total dissolved carbon concentration of the brine initially equilibrated with the mineralogical assemblage, before CO_2 "injection") are of the order of 0.01% or less for precipitating minerals (quartz, dolomite, anhydrite) and less than 0.08% for dissolving ones (siderite, calcite). Another indicator of this low impact on the mineralogical assemblage is the negligible porosity variation observed on Figure 12f. Lastly, it can be observed on Figure 12g that pH remains constant at a value of 4.2 which is not surprising due to the

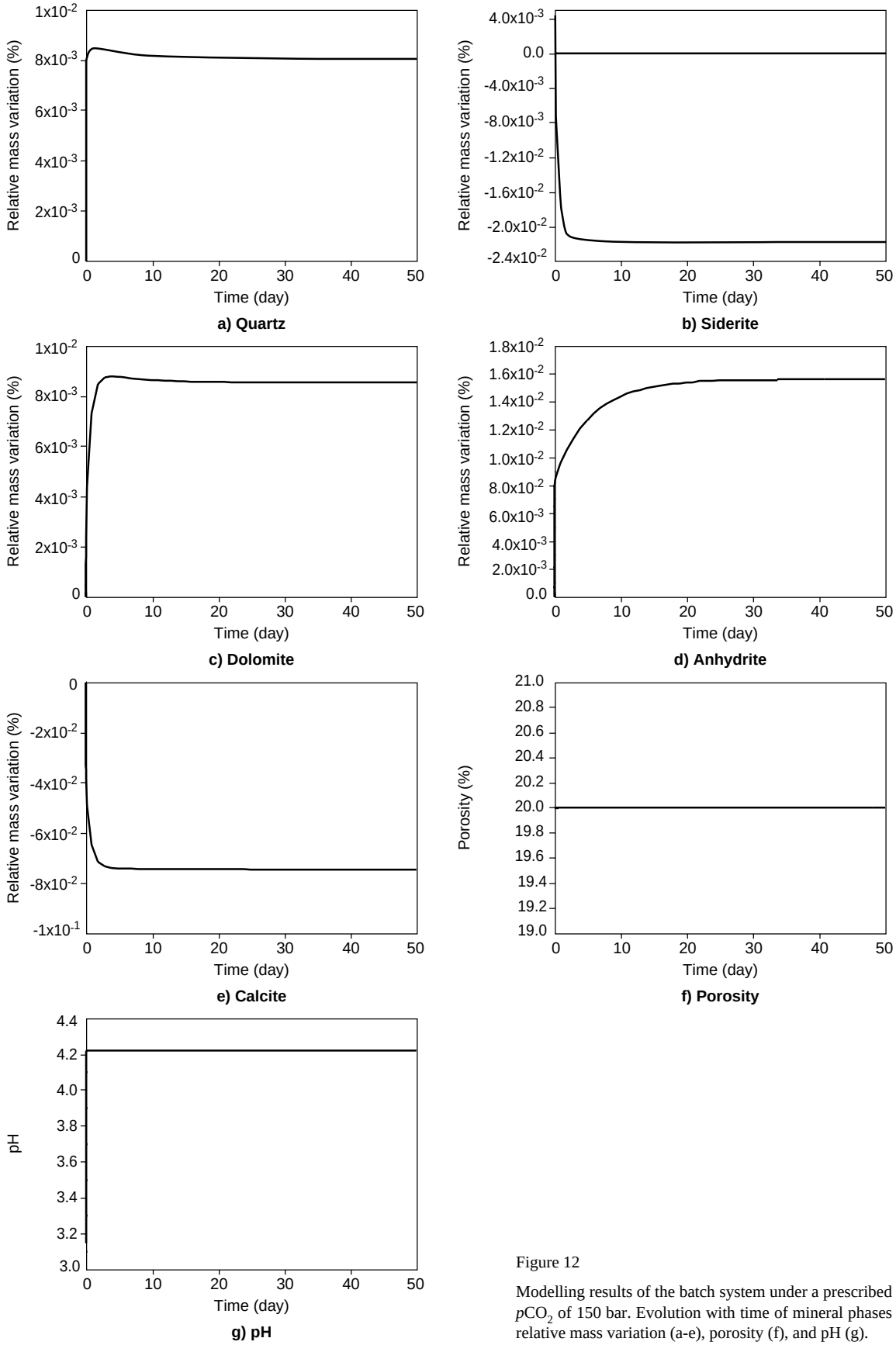

Figure 12

Modelling results of the batch system under a prescribed pCO_2 of 150 bar. Evolution with time of mineral phases relative mass variation (a-e), porosity (f), and pH (g).

buffering effect induced by the presence of carbonates; however, looking more in details at the result file show a rapid initial increase in pH from 3.1 to 4.2 in less than 0.5 day (not visible on Figure 12g). This is a response to the dramatic initial change in CO_2 partial pressure varying instantaneously from 0.382 bar (initial "S4" water in Table 1, corresponding to a fugacity of 0.203 bar) to 150 bar (fugacity of 79.8 bar) and to the simultaneous dissolution/precipitation of carbonate minerals.

However, this batch simulation has to be considered as a first convenient way of evaluating qualitatively the potential impact of a high dissolved CO_2 concentration on a geochemical system. By definition, such a closed reactor at fixed pressure and temperature conditions, has a limited capacity to dissolve CO_2 and once gas-water-mineral equilibrium is reached, nothing else is going to happen. Moreover, CO_2 injection in an aquifer is by nature a dynamical process. It is then essential to be able to consider the combined effects of both fluid dynamics and chemical reactions, which is much more intricate in terms of physical processes and numerical aspects. SCALE2000 enables the simulation of coupled chemistry and mass transfer using a specific approach based on a set of perfectly mixed reactors connected in series. Originally, this option was implemented for simulating scale deposition along production or injection wells in oil or geothermal fields. Further details on this concept which enables 1D chemistry-transport coupled modelling, and on the basic equations, can be found in Azaroual *et al.* (2004a, 2004c). A diagram of the set of reactors and the initial and boundary conditions are presented on Figure 13. For comparison with batch calculation, we first focused on a single reactor (reactor no. 1) identical to the batch reactor presented above in terms of total volume (5 l), initial water-rock ratio (1:4 in volume), and initial chemical composition (fluid + minerals). Similarly to what was done for the batch reactor, we prescribed a constant pCO_2 of 150 bar in reactor no. 1 for the whole simulation duration (50 y). However, we considered here that the system was continuously fed by an injection fluid at a constant flow rate (corresponding to an initial pore water velocity of 1 m·day^{-1}), the chemical composition of this injection fluid being identical to that of the brine initially present in the reactors (*i.e.* fluid "S4" in *Table 1*).

All things being equal initially, the results presented on Figure 14 demonstrate the impact of mass transport on the geochemical evolution of the system: the continuous fluid renewal has a dramatic effect on the geochemistry of the system and no steady state can be reached after a simulated

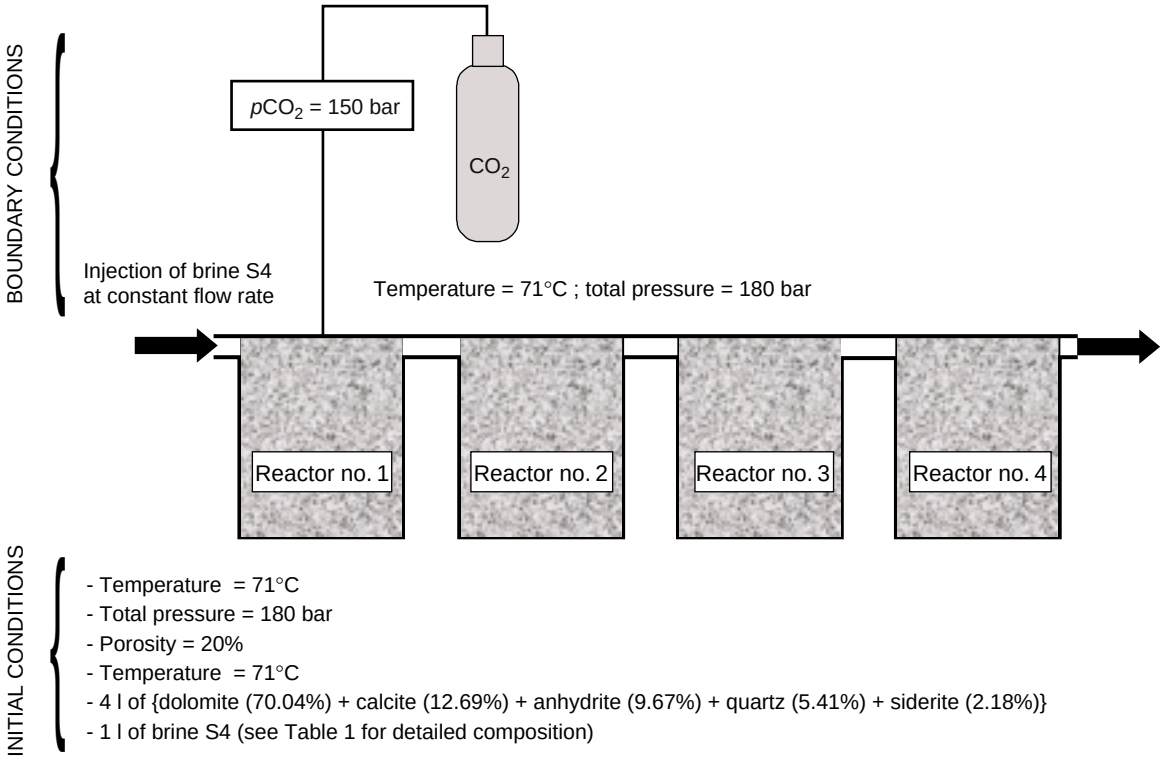

Figure 13

Diagram of the open-reactor system constituted of four identical homogeneous reactors connected in series. This configuration enables to simulate 1D chemistry-transport coupled processes. Initial and boundary conditions are detailed.

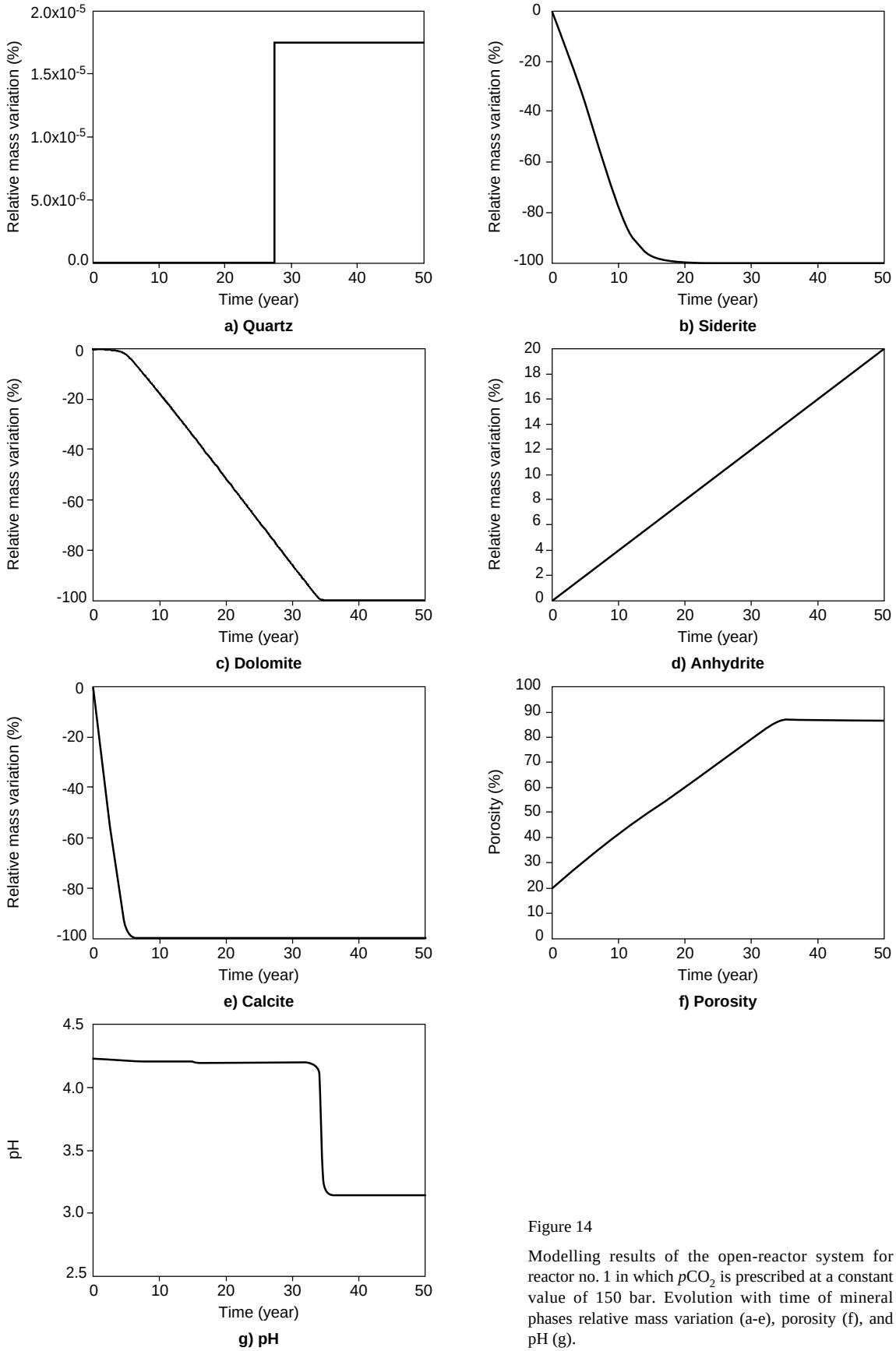

Figure 14

Modelling results of the open-reactor system for reactor no. 1 in which pCO_2 is prescribed at a constant value of 150 bar. Evolution with time of mineral phases relative mass variation (a-e), porosity (f), and pH (g).

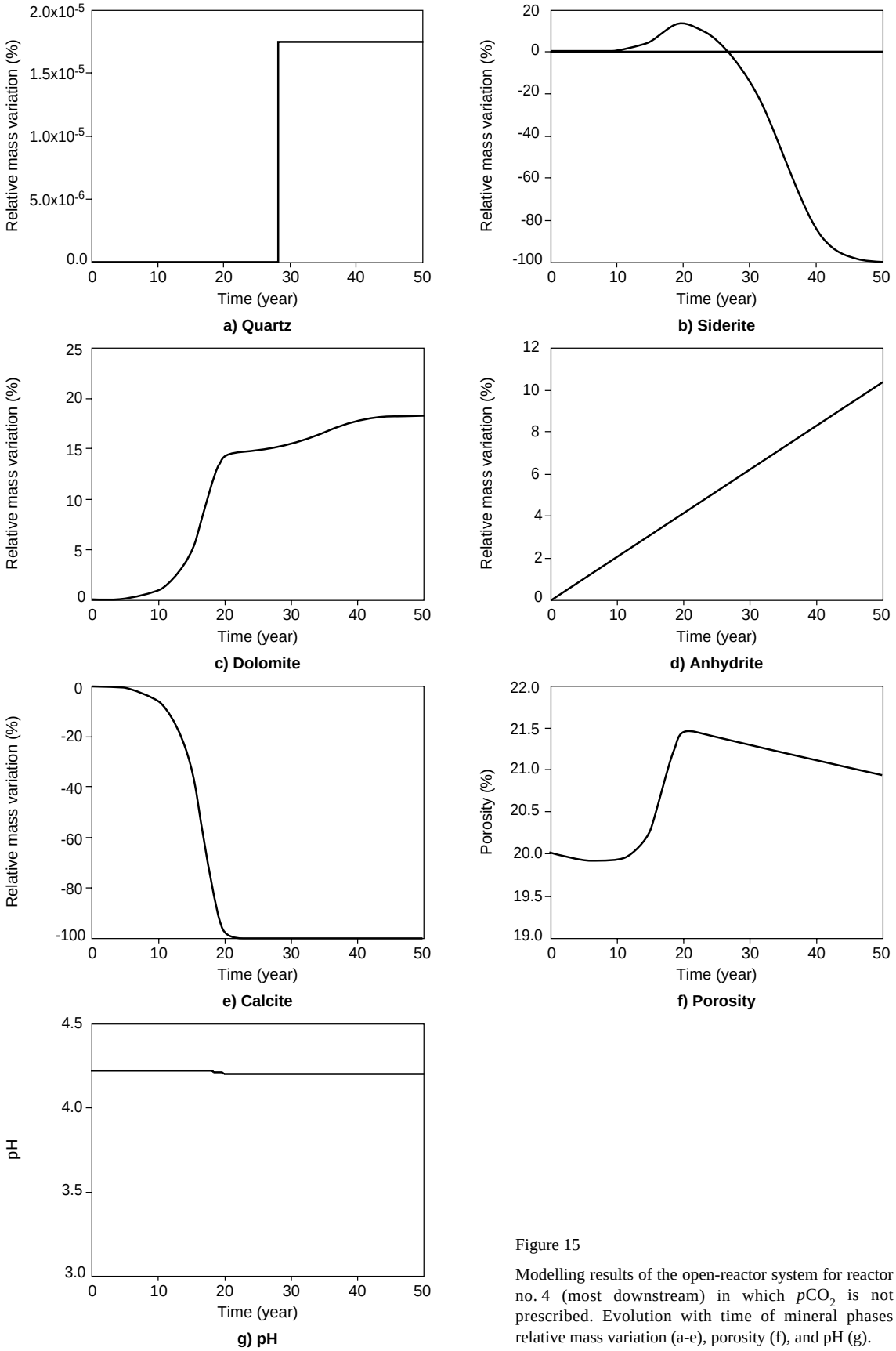

Figure 15

Modelling results of the open-reactor system for reactor no. 4 (most downstream) in which pCO_2 is not prescribed. Evolution with time of mineral phases relative mass variation (a-e), porosity (f), and pH (g).

period of 50 y, whereas thermodynamic equilibrium was reached in a few tens of days only for the batch reactor case. The mineral composition now appears to be strongly modified with respect to the initial state (detailed in *Table 2*): all carbonated minerals (calcite, siderite, and dolomite) are exhausted from the system in less than 35 y *(Figs 14b, 14c, 14e)*. The disappearing of all carbonates results in a loss of the buffering capacity of the system illustrated by the sudden decrease in pH from 4.2 to 3.14 *(Fig. 14g)* observed as soon as the last carbonate species (dolomite) has totally dissolved; pH is then directly controlled by the high partial pressure of CO_2 (150 bar). In the meanwhile, quartz can be considered as inert even though some negligible precipitation can be observed *(Fig. 14a)*. Anhydrite precipitates continuously at a constant rate *(Fig. 14d)* independently of carbonates dissolution and pH variation. This indicates that the common ion effect (Ca provided by calcite and dolomite dissolution) does not influence the precipitation rate of anhydrite. As a consequence of these dissolutions and because amounts of precipitated anhydrite remains relatively weak, porosity strongly varies from an initial value of 20% to above 85% within the first 30 y of simulation and then remains approximately constant.

This very high increase in porosity is in contrast to the mineral trapping effect that one might expect to occur when injecting CO_2 in a reservoir. However, being in a carbonated reservoir under constant high CO_2 pressure conditions, this behaviour could have been predicted beforehand. Nevertheless, it is interesting to compare the behaviour of the system of reactors studied here to the results obtained in Bonijoly *et al.* (2003). In this work, 1D finite difference coupled simulations of CO_2 injection in the carbonated Dogger aquifer (Paris Basin, France) were performed and high rates of calcite dissolution, leading to a huge increase in porosity, were also observed in the immediate vicinity of the injection well. At the same time, calcite reprecipitation (thus inducing some CO_2 trapping) was observed a few tens of metres upstream the injection well (where it has to be noticed

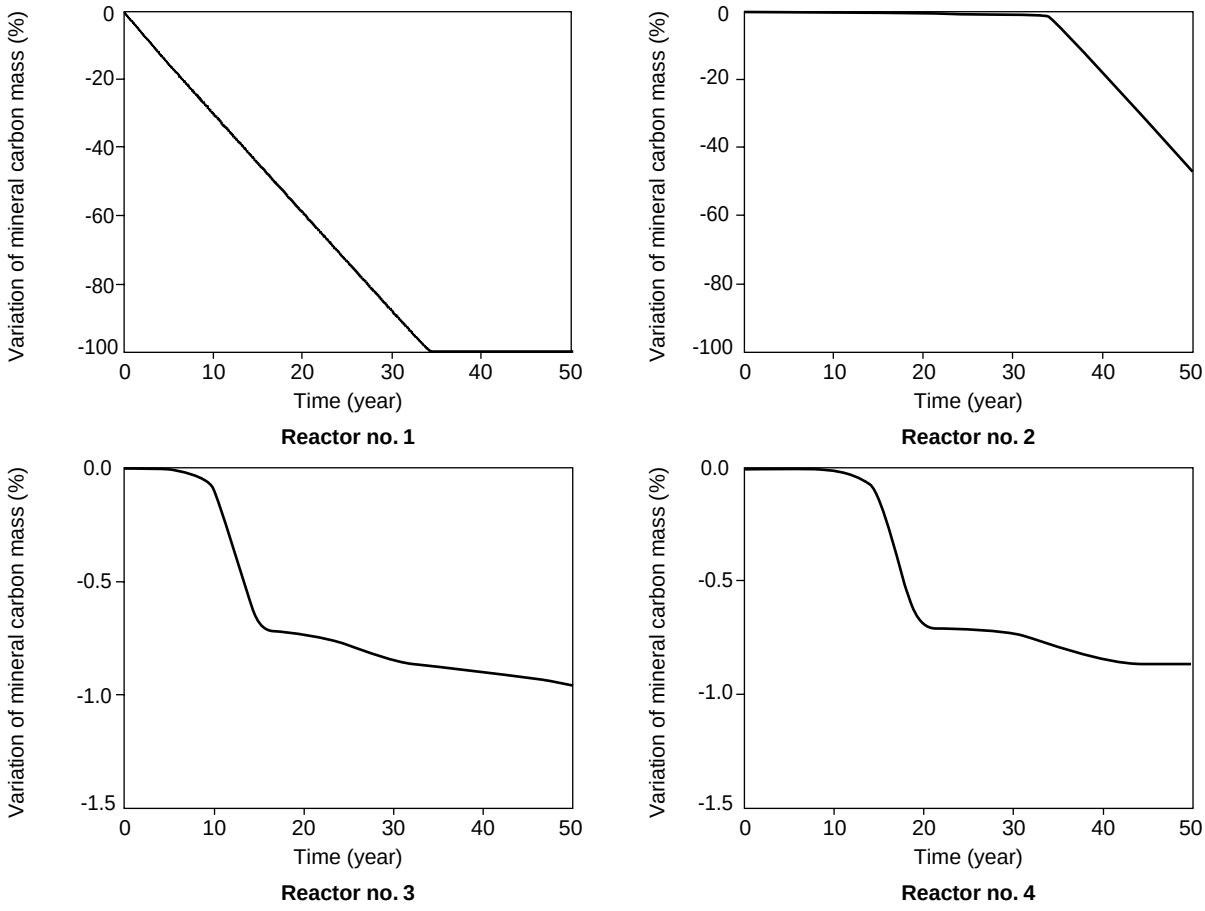

Figure 16

Modelling results of the 1D system constituted of a set of four identical homogeneous reactors connected in series. Relative variation of mineral carbon mass (mole of representative elementary volume of saturated bulk rock) in the four reactors of the system (from upstream to downstream). In reactor no. 1 (most upstream), pCO_2 is prescribed (150 bar); in the three other reactors, pCO_2 is not prescribed.

that the temperature was higher). In the present study with SCALE2000, where calculations were carried out on a set of four identical reactors connected in series (pCO_2 being prescribed in reactor no. 1 only) at constant temperature and pressure, it is interesting to remark that in the most-downstream reactor (*i.e.* reactor no. 4, see *Fig. 13*), while siderite and calcite also disappeared (with noticeable retardation with respect to reactor no. 1), significant dolomite precipitation can be observed as illustrated on Figure 15, suggesting some possible carbon mineral trapping. In reactor no. 4, porosity variations are almost negligible in comparison to what was observed in reactor no. 1.

In order to investigate the possible trapping capacity of the studied system, we performed carbon mass balance calculations for the whole simulated period (50 y). For that purpose, we calculated in the four reactors the total amounts of carbon trapped in the mineral phases. Figure 16 show the corresponding results expressed in terms of relative mass variation of carbon stored in carbonates (calcite, dolomite, and siderite) with respect to the initial amounts (as detailed in *Table 2*). Confirming what was observed in Figure 14, all mineral carbon was removed from reactor no. 1 (variation of –100%) after 35 y. In reactor no. 2, only 50% of the initial carbon in solid was dissolved; however, the general trend suggest a similar tendency than in reactor no. 1, *i.e.* total dissolution of mineral carbon, with a retardation factor of about 35 y. More surprising are the results obtained for reactors no. 3 and no. 4 where mineral carbon dissolution is here considerably less important (less than 1% of the initial mass), due to significant dolomite precipitation (see *Fig. 15*). The net carbon mass balance over the four reactors is thus largely negative, however, the trend shown in the last two reactors may let us expect a positive mass balance (*i.e.* actual carbon trapping in carbonates) beyond the fourth reactor considered here. As mentioned earlier, this behaviour can be favourably compared to modelling results obtained by Bonijoly *et al.* (2003) where carbonates precipitation was predicted a few tens of metres downstream the injection well. The space scale considered here (a set of four 5 l total capacity reactors) is obviously incomparable to the site scale. Consequently, further modelling work should be carried out at a scale of at least a few hundred metres around the "injection point", thus requiring the use of more sophisticated numerical tools enabling 1D, 2D, or even 3D hydrodynamics-transport-chemistry coupled modelling. Relying on the coupling approach presented in Kervévan *et al.* (1998), this could possibly be achieved through interfacing the SCALE2000 geochemical calculation modules with a 1D, 2D, or 3D hydrodynamics and mass transport code. Provided that a detailed mineralogical description of the site would also be available, it might then be possible to draw more definitive conclusions on the actual mineral trapping capacity of a carbonated formation such as Smackover.

CONCLUSION

This work presents some improvements for brine-rock-gas interaction modelling through the inclusion of thermodynamic approaches specifically dedicated to high salinity, high pressure, and high temperature conditions. These formalisms were all implemented in the thermo-kinetic modelling software SCALE2000 (Azaroual *et al.*, 2004a). They mainly deal with activity correction for dissolved species (25-250°C, 1-1000 bar, ionic strength up to 6 M) and density calculation involving Pitzer's formalism (Monnin, 1994), the taking into account of the influence of both temperature and pressure (particularly at high pressure conditions) on thermodynamic equilibrium constants, and fugacity coefficient correction based on Duan *et al*'s. (1992a, 1992b, 2003) equations of state. They enable to calculate more accurately CO_2 solubility in brines, which is obviously a key parameter in the context of CO_2 injection studies.

A quantification of the relative weight of each of these corrections was proposed and it appears that fugacity and activity corrections have the greatest impact on the precision of the geochemical calculations applied to a CO_2-brine-minerals system under conditions of relatively high temperature, pressure, and salinity, which are likely to be encountered at potential CO_2 sequestration sites.

On the basis of these developments recently integrated in SCALE2000, we presented in the second part of this paper an example of application to a hypothetical scenario of massive CO_2 injection in a carbonated formation, considering actual geochemical data from the Smackover site (Arkansas, United State) for the brine composition (Moldovanyi and Walters, 1992). The purpose of these calculations was to evaluate the geochemical impact on both mineral and fluid compositions of a high prescribed CO_2 pressure (150 bar). The first series of simulations for a representative elementary volume of saturated bulk rock considered as a closed system (batch reactor), showed a relatively short response time (a few tens of years) but finally demonstrated a relatively low impact of the presence of CO_2 on the mineral composition. A second series of simulations performed on the same initial representative elementary volume of bulk rock, now considered as a single open reactor crossed by a constant water flow rate, led to dramatic changes in the mineral composition at the end of our 50 y simulation: carbonated minerals (calcite, dolomite, siderite), initially present in large amounts, totally disappeared while anhydrite precipitated continuously. As a consequence, a strong increase in porosity was observed (variation from 20 to 85%) thus suggesting a poor mineral trapping capacity of the system. However, further calculations carried out with SCALE2000, now considering an approximated 1D system constituted of a set of four homogeneous identical reactors, showed significant dolomite precipitation in the most-downstream reactor and hence, some CO_2 precipitation. First mass balance

calculations performed on the four reactors system finally showed a global loss in total mineral carbon with respect to initial conditions. However, the trend in the most-downstream two reactors indicated that possible trapping might be expected beyond the considered geometrical limit of our modelled system. This behaviour can be favourably compared to observations made in the study by Bonijoly *et al.* (2003) on CO_2 injection in the carbonated Dogger aquifer (Paris Basin) where high porosity increase was also predicted near the injection well while carbonates precipitation was calculated by the 1D coupled model a few tens of metres downstream. However, drawing more definitive conclusions on the mineral trapping capacity of the Smackover formation would necessitate further simulations at the site scale considering, in particular, a more detailed mineralogical description and a sophisticated hydrodynamic and mass transfer model (1D, 2D, or 2D) more adapted to deal with complexity of the physics of gas injection and flow in aquifers.

ACKNOWLEDGEMENTS

This work was supported by both the French project PICOR on CO_2 trapping in reservoirs and the *Research Directorate* of *BRGM* ("Hydrogeological and Coupling Modelling" project). We would like to thank the PICOR partners for authorising us to publish these results. We are also grateful to E.H. Perkins, M. Kühn, É. Brosse, and one anonymous reviewer who greatly helped us to improve the original manuscript.

Note: In agreement with the editor, proprietary data, not essential for an understanding of the principles underlying the calculations, are not divulged in this article.

REFERENCES

Aagaard, P. and Helgeson, H.C. (1982) Thermodynamic and Kinetic Constraints on Reaction Rates Among Minerals and Aqueous Solutions. I. Theoretical Considerations. *American Journal of Science*, **282**, 237-285.

Azaroual, M., Kervévan, C., Durance, M.V., Brochot, S. and Durst, P. (2004a) SCALE2000 (V3.1), *User's Manual* (in French), BRGM. ISBN 2-7159-0939-X.

Azaroual, M., Durst, P., Czernichowski-Lauriol, I., Olsen, D.N., Springer, N., Rochelle, C.A., Pearce, J., Bateman, K. and Birchall, D. (2004b) Geochemical Reactions Resulting from CO_2 Injection into the Midale Formation, Weyburn Oilfield; A Laboratory Experimental and Modelling Study. *Abstract Submitted to GHGT7 - 7th International Conference on Greenhouse Gas Control Technologies*, Vancouver, Canada, 5-9 September.

Azaroual, M., Kervévan, C., Durance, M.V. and Durst, P. (2004c) SCALE2000: A Reaction-Transport Software Dedicated to Thermo-Kinetic Prediction and Quantification of Scales. Applicability to Desalination Problems. *Desalination*, **156**, 409-419.

Bonijoly, D., Barbier, J., Robelin, C., Kervévan, C., Thiéry, D., Menjoz, A., Matray, J.M., Cotiche, C. and Herbrich, B. (2003) Feasibility of CO_2 Storage in Geothermal Reservoirs. Example of the Paris Basin - France. BRGM-CFG-ANTEA Contribution to the GESTCO Project. *BRGM Report RP-52349-FR*.

Czernichowski-Lauriol, I., Rochelle, C.A., Brosse, É., Springer, N., Pearce, J.M., Bateman, K.A., Sanjuan, B. and Kervévan, C. (2001) Disposal of CO_2 in Deep Aquifers: Investigations of Water-Rock-CO_2 Interactions at Sleipner (North Sea) Within the SACS Project. *EUG XI*, 8-12 April, Strasbourg.

Demir, I. and Seyler, B. (1999) Chemical Composition and Geologic History of Saline Waters in Aux Vases and Cypress Formations, Illinois Basin. *Aquatic Geochemistry*, **5**, 281-311.

Drummond, S.E. (1981) Boiling and Mixing of Hydrothermal Fluids: Chemical Effects on Mineral Precipitation. *PhD Thesis*, Pennnsylvania State University.

Duan, Z., Moller, N. and Weare, J.H. (1992a) An Equation of State for the CH_4-CO_2-H_2O System: I. Pure Systems for 0 to 1000°C and 0 to 8000 bar. *Geochimica et Cosmochimica Acta*, **56**, 2605-2617.

Duan, Z., Moller, N. and Weare, J.H. (1992b) An Equation of State for the CH4-CO2-H2O System: II. Mixture from 50 to 1000°C and 0 to 1000 bar. *Geochimica et Cosmochimica Acta*, 56, 2619-2631.

Duan, Z. and Sun, R. (2003) An Improved Model Calculating CO_2 Solubility in Pure Water and Aqueous NaCl Solutions from 273 to 5333 K and from 0 to 2000 bar. *Chemical Geology*, **193**, 257-271.

Gaus, I., Azaroual, M. and Czernichowski-Lauriol, I. (2005) Reactive Transport Modelling of the Impact of CO_2 Injection on the Clayey Cap Rock at Sleipner (North Sea). *Chemical Geology* (in press).

Gunter, W.D., Wiwchar, B. and Perkins, E.H. (1997) Aquifer Disposal of CO_2-rich Greenhouse Gases: Extension of the Time Scale of Experiment for CO_2-Sequestering Reactions by Geochemical Modelling. *Mineralogical Petrology*, **59**, 121-140.

Harvie, C.E., Moller, N. and Weare, J.H. (1984) The Prediction of Mineral Solubilities in Natural Waters: The Na-K-Mg-Ca-H-Cl-SO_4-OH-HCO_3-CO_3-CO_2-H_2O System to High Ionic Strengths at 25°C. *Geochimica et Cosmochimica Acta*, **48**, 723-751.

Helgeson, H.C., Kirkham, D.H. and Flowers, G.C. (1981) Theoretical Prediction of the Thermodynamic Behavior of Aqueous Electrolytes by High Pressures and Temperatures; IV, Calculation of Activity Coefficients, Osmotic Coefficients, and Apparent Molal and Standard and Relative Partial Molal Properties to 600°C and 5 kb. *American Journal of Science*, **281**, 10, 1249-1516.

Hitchon, B., Billings, G.K. and Klovan, J.E. (1971) Geochemistry and origin of Formation Waters in the Western Canada Sedimentary Basin - III. Factors Controlling Chemical Composition. *Geochemica et Cosmochemica Acta*, **35**, 567-598.

Johnson, J.W., Oelkers, E.H. and Helgeson, H.C. (1992) SUPCRT92; a Software Package for Calculating the Standard Molal Thermodynamic Properties of Minerals, Gases, Aqueous Species, and Reactions from 1 to 5000 bar and 0 to 1000 Degrees C. *Computers and Geosciences*, **18**, 7, 899-947.

Kaszuba, J.P., Janecky, D.R. and Snow, M.G. (2003) Carbon Dioxide Reaction Processes in a Model Brine Aquifer at 200°C and 200 bar: Implications for Geologic Sequestration of Carbon. *Applied Geochemistry*, **18**, 1065-1080

Kelly, W.C., Rye, R.O. and Livnat, A. (1986) Saline Minewaters of the Keweenaw Peninsula, Northern Michigan: their Nature, Origin, and Relation to Similar Deep Waters in Precambrian Crystalline Rocks of the Canadian Shield. *American Journal of Sciences*, **286**, 281-308.

Kervévan, C., Thiéry, D. and Baranger, P. (1998) SCS: Specific Chemical Simulators Dedicated to Chemistry-transport Coupled Modelling: Part III. Coupling of SCS with the Hydro-transport

Modelling Software MARTHE. *Mineralogical Magazine*, **62A**, 773-774.

Kharaka, Y.K., Gunter, W.D., Aggarwal, P.K., Perkins, E.H. and De Braal, J.D. (1988) SOLMINEQ.88: A Computer Program Code for Geochemical Modeling of Water-Rock Interactions. *US Geological Survey Water-Resources Investigations, Report 88-4227.*

Land, L.S. (1995) Na-Ca-Cl Saline Formation Waters, Frio Formation (Oligocene), South Texas, USA: Products of Diagenesis. *Geochemica et Cosmochemica Acta*, **59**, 11, 2163-2174.

Langmuir, D. and Melchior, D. (1985) The Geochemistry of Ca, Sr, Ba and Ra Sulfates in some Deep Brines from the Palo Duro Basin, Texas. *Geochemica et Cosmochemica Acta*, **49**, 2423-2432.

Lasaga, A.C. (1984) Chemical Kinetics of Water-Rock Interactions. *Journal of Geophysical Research*, **89**, 4009-4025.

Leach, D.L., Plumlee, G.S., Hofstra, A.H., Landis, G.P., Rowan, E.L. and Viets, J.G. (1991) Origin of Late Dolomite Cement by CO_2-saturaed Deep Basin Brines: Evidence from the Ozark Region, Central United States. *Geology*, **19**, 348-351.

Lee, B.I. and Kesler, M.G. (1975) A Generalised Thermodynamic Correlation Based on Three-Parameter Corresponding States. *American Institute of Chemical Engineers Journal*, **21**, 510-527.

Malinin, S.D. and Kurovskaya, N.A. (1975) The Solubility of CO_2 in Chloride Solutions at Elevated Temperatures and CO_2 Pressures. *Geochem. Int.*, **12**, 199-201.

Martel, A.T., Gibling, M.R. and Nguyen, M. (2001) Brines in the Carboniferous Sydney Coalfield, Atlantic Canada. *Applied Geochemistry*, **16**, 35-55.

Moldovanyi, E.P. and Walter, L.M. (1992) Regional Trends in Water Chemistry, Smackover Formation, Southwest Arkansas: Geochemical and Physical Controls. *American Association of Petroleum Geologists Bulletin*, **76**, 864-894.

Monnin, C. (1990) The Influence of Pressure on the Activity Coefficients of the Solutes and on the Solubility of Minerals in the System Na-Ca-Cl-SO_4-H_2O to 200°C and 1 kbar and to High NaCl Concentration. *Geochimica et Cosmochimica Acta*, **54**, 3265-3282.

Monnin, C. (1994) Density Calculation and Concentration Scale Conversions for Natural Waters. *Computers and Geosciences*, **20**, 1435-1445.

Parkhurst, D.L. and Appelo, C.A.J. (1999) User's guide to PHREEQC (version 2) -A computer program for speciation, batch-reaction, one-dimensional transport, and inverse geochemical calculations, *US Geological Survey Water-Resources Investigations, Report 99-4259.*

Pitzer, K.S. (1973) Thermodynamics of Electrolytes. I. Theoretical Basis and General Equations. *Journal of Physical Chemistry*, **12**, 268-277.

Rumpf, B. and Maurer, G. (1993) An Experimental and Theoretical Investigation on the Solubility of Carbon Dioxide in Aqueous Solutions of Strong Electrolytes. *Berichte der Bunsen-Gesellschaft - Physical Chemistry*, **97**, 85-97.

Stueber, A.M., Saller, A.H. and Ishida, H. (1998) Origin, Migration, and Mixing of Brines in the Permian Basin: Geochemical Evidence from the Eastern Central Basin Platfrom, Texas. *American Association of Petroleum Geologists Bulletin*, **82**, 9, 1652-1672.

Takenouchi, S. and Kennedy, G.C. (1964) The Solubility of Carbon Dioxide in NaCl Solution at High Temperatures and Pressures. *American Journal of Science*, **263**, 445-454.

Wolery, T.J. (1992) *EQ3/6, a Software Package for Geochemical Modeling of Aqueous Systems: Package Overview and Installation Guide (version 7.2b)*, Lawrence Livermore National Laboratory, Livermore, California.

Xu, T., Apps, J.A. and Pruess, K. (2004) Numerical Simulation of CO_2 Disposal by Mineral Trapping in Deep Aquifers. *Applied Geochemistry*, **19**, 917-936.

Yasunichi, Y. and Yoshida, F. (1979) Solubility of Carbon Dioxide in Aqueous Electrolyte Solutions. *Journal of Chemical Engineering Data*, **24**, 11-14.

Final manuscript received in January 2005

Copyright © 2005, Institut français du pétrole

Permission to make digital or hard copies of part or all of this work for personal or classroom use is granted without fee provided that copies are not made or distributed for profit or commercial advantage and that copies bear this notice and the full citation on the first page. Copyrights for components of this work owned by others than IFP must be honored. Abstracting with credit is permitted. To copy otherwise, to republish, to post on servers, or to redistribute to lists, requires prior specific permission and/or a fee: Request permission from Documentation, Institut français du pétrole, fax. +33 1 47 52 70 78, or revueogst@ifp.fr.

APPENDIX 1

PHREEQC input file used for the series of calculations performed considering a 1 M NaCl solution at 150°C and pressures varying from 50 to 400 bar (see *Section 1.5* for details). Corresponding results are represented on Figure 8.

Database used is llnl.dat (revision 1.11) based on the Davies activity model which is enabled adding "#" at the beginning of every "-llnl gamma" command line.

PHREEQC without Fugacity Correction

```
Solution 1
   temp          150
   pH            7
   pe            4
   redox         pe
   units         mol/kgw
   density       1
   Na            1
   Cl            1
   water         1 # kg
Gas phase 1
   fixed pressure
   pressure      50
   volume        10
   temperature   150
   CO2(g)        50
End
Use solution     1
Gas phase        1
   fixed pressure
   pressure      100
   volume        10
   temperature   150
   CO2(g)        100
End
Use solution     1
Gas phase        1
   fixed pressure
   pressure      150
   volume        10
   temperature   150
   CO2(g)        150
End
Use solution 1
Gas phase 1
   fixed pressure
   pressure      200
   volume        10
   temperature   150
   CO2(g)        200
End
Use solution     1
Gas phase        1
   fixed pressure
   pressure      250
   volume        10
   temperature   150
   CO2(g)        250
End
Use solution     1
Gas phase        1
   fixed pressure
   pressure      300
   volume        10
   temperature   150
   CO2(g)        300
End
Use solution     1
Gas phase        1
   fixed pressure
   pressure      350
   volume        10
   temperature   150
   CO2(g)        350
End
Use solution     1
Gas phase        1
   fixed pressure
   pressure      400
   volume        10
   temperature   150
   CO2(g)        400
End
```

PHREEQC with Fugacity Correction

```
Solution 1
   temp          150
   pH            7
   pe            4
   redox         pe
   units         mol/kgw
   density       1
   Na            1
   Cl            1
   water         1 # kg
Gas phase 1
   fixed pressure
   pressure 46.6119   #50 bar
   volume        10
   temperature   150
   CO2(g)        46.6119
End
```

```
Use solution 1
Gas phase 1
    fixed pressure
    pressure 86.8065    #100 bar
    volume              10
    temperature         150
    CO2(g)              86.8065
End
Use solution 1
Gas phase 1
    fixed pressure
    pressure 121.6580   #150 bar
    volume              10
    temperature         150
    CO2(g)              121.6580
End
Use solution 1
Gas phase 1
    fixed pressure
    pressure 152.39     #200 bar
    volume              10
    temperature         150
    CO2(g)              152.39
End
Use solution 1
Gas phase 1
    fixed pressure
    pressure 180.3845   #250 bar
    volume              10
    temperature         150
    CO2(g)              180.3845
End
Use solution 1
Gas phase 1
    fixed pressure
    pressure 206.9495   #300 bar
    volume              10
    temperature         150
    CO2(g)              206.9495
End
Use solution 1
Gas phase 1
    fixed pressure
    pressure 233.0895   #350 bar
    volume              10
    temperature         150
    CO2(g)              233.0895
End
Use solution 1
Gas phase 1
    fixed pressure
    pressure 259.4746   #400 bar
    volume              10
    temperature         150
    CO2(g)              259.4746
End
```

APPENDIX 2

PHREEQC input file used for the initial speciation calculations based on the Smackover brine data of Moldovanyi and Walters (1992) (see *Section 2.1* for details). Corresponding results are detailed in Table 1.

Database used is llnl.dat (revision 1.11) based on the Davies activity model which is enabled adding "#" at the beginning of every "-llnl gamma" command line.

```
Solution 1
    temp        25
    pe          4
    redox       pe
    units       mg/l
    density     1.132
    acetate     0.25 mmol/l
    alkalinity  3.65 meq/l
    B           54
    Br          2206
    Ca          17 825
    Cl          120 050 charge
    Fe          23
    K           560
    Li          21
    Mg          2482
    Mn          0
    Na          51 675
    F           10
    I           24
    S           425 as SO4
    Si          28 as SiO2
    Sr          732
    C           3.45 mmol/l
Reaction temperature
    71.0
Equilibrium phases
    CO2(g)  1.902 10   #pCO2 = fCO2 = 79.8 bar
End
```